

Lepton-flavor violation via right-handed neutrino Yukawa couplings in the supersymmetric standard model

J. Hisano,^{1,2} T. Moroi,^{3,4} K. Tobe,^{5,6} and M. Yamaguchi⁶

¹*Tokyo Institute of Technology, Department of Physics, Oh-okayama, Meguro, Tokyo 152, Japan*

²*Institute for Theoretical Physics, University of California, Santa Barbara, California 93106*

³*Theory Group, KEK, Ibaraki 305, Japan*

⁴*Theoretical Physics Group, Lawrence Berkeley Laboratory, University of California, Berkeley, California 94720*

⁵*Department of Physics, University of Tokyo, Tokyo 113, Japan*

⁶*Department of Physics, Tohoku University, Sendai 980-77, Japan*

(Received 16 October 1995)

Various lepton-flavor-violating (LFV) processes in the supersymmetric standard model with right-handed neutrino supermultiplets are investigated in detail. It is shown that large LFV rates are obtained when $\tan\beta$ is large. In the case where the mixing matrix in the lepton sector has a similar structure as the Kobayashi-Maskawa matrix and the third-generation Yukawa coupling is as large as that of the top quark, the branching ratios can be as large as $B(\mu \rightarrow e\gamma) \approx 10^{-11}$ and $B(\tau \rightarrow \mu\gamma) \approx 10^{-7}$, which are within the reach of future experiments. If we assume a large mixing angle solution to the atmospheric neutrino problem, the rate for the process $\tau \rightarrow \mu\gamma$ becomes larger. We also discuss the difference between our case and the case of the minimal SU(5) grand unified theory.

PACS number(s): 12.60.Jv, 11.30.Hv, 12.15.Ff

I. INTRODUCTION

Lepton-flavor-violation (LFV), if observed in a future experiment, is evidence of new physics beyond the standard model, because the lepton-flavor number is conserved in the standard model. Since the processes do not suffer from a large ambiguity due to hadronic matrix elements, a detailed analysis of the LFV processes will reveal some properties of high-energy physics.

One of the minimal extensions of the standard model with LFV is the model with nonvanishing neutrino masses. If the masses of the neutrinos are induced by the seesaw mechanism [1], one has a new set of Yukawa couplings involving right-handed neutrinos. The introduction of the new Yukawa couplings generally gives rise to flavor violation in the lepton sector, similar to its quark sector counterparts. In nonsupersymmetric standard models, however, the amplitudes of the LFV processes are proportional to inverse powers of the right-handed neutrino mass scale which is typically much higher than the electroweak scale, and as a consequence such rates are highly suppressed.

If the model is supersymmetrized, the situation becomes quite different. LFV in right-handed neutrino Yukawa couplings leads to LFV in slepton masses through renormalization-group effects [2]. Then the LFV processes are only suppressed by powers of supersymmetry- (SUSY-) breaking scale which is assumed to be at the electroweak scale. Especially, in a previous paper [3], we pointed out that a large left-right mixing of the slepton masses greatly enhances the rates for LFV processes such as $\mu \rightarrow e\gamma$ and $\tau \rightarrow \mu\gamma$. Because of this effect, they can be within the reach of near future experiments even if the mixing angle of the lepton sector is as small as that of the quark sector.

In this paper, we will extend the previous analysis. We are interested in the processes $\mu \rightarrow e\gamma$, $\tau \rightarrow \mu\gamma$, $\mu \rightarrow eee$, and μ - e conversion in nuclei, and calculate formulas for the interaction rates of the above processes. In our calculation, we fully incorporate the mixing of the slepton masses as well as the mixings in the neutralino and chargino sectors. Also the lepton Yukawa couplings in Higgsino-lepton-slepton vertices are retained, which yield another type of enhanced diagram in the large $\tan\beta$ region. Then we will discuss how large the interaction rates can be, assuming the radiative electroweak symmetry-breaking scenario [4]. We find that a large value of $\tan\beta$ is realized with a relatively light superparticle mass spectrum, and thus the interaction rates can indeed be enhanced. For the right-handed neutrino sector, we will mainly consider the case where the Yukawa couplings of the right-handed neutrinos are similar to those of the up-type quarks. We will also discuss the case of large mixing between second and third generations, suggested by the atmospheric neutrino problem. In our numerical analysis, we impose constraints from negative searches for SUSY particles, as well as the constraint from the muon anomalous magnetic dipole moment $g-2$ to which superparticle loops give non-negligible contributions especially in the large $\tan\beta$ region.

The organization of our paper is as follows. In the subsequent section, we will review LFV in slepton masses in the presence of right-handed neutrinos. In Sec. III, we will give formulas of the interaction rates of the various LFV processes. The results of our numerical study are given in Sec. IV. In Sec. V, after summarizing our results, we will compare our case with the case of SU(5) grand unification briefly. Renormalization-group equations relevant to our analysis are summarized in Appendix A. In Appendix B, we describe the interactions among neutralinos (charginos), fermions, and

sfermions. In Appendix C, we will give formulas of the SUSY contribution to $g-2$.

II. LFV IN SCALAR LEPTON MASSES

Throughout this paper, we consider the minimal SUSY standard model (MSSM) plus three-generation right-handed neutrinos. In this case, the superpotential is given by

$$W = f_l^{ij} \epsilon_{\alpha\beta} H_1^\alpha E_i^c L_j^\beta + f_\nu^{ij} \epsilon_{\alpha\beta} H_2^\alpha N_i^c L_j^\beta + f_d^{ij} \epsilon_{\alpha\beta} H_1^\alpha D_i^c Q_j^\beta + f_u^{ij} \epsilon_{\alpha\beta} H_2^\alpha U_i^c Q_j^\beta + \mu \epsilon_{\alpha\beta} H_1^\alpha H_2^\beta + \frac{1}{2} M_\nu^{ij} N_i^c N_j^c, \quad (1)$$

where L_i represents the chiral multiplet of an $SU(2)_L$ doublet lepton, E_i^c an $SU(2)_L$ singlet charged lepton, N_i^c a right-handed neutrino which is singlet under the standard-model

gauge group and H_1 and H_2 two Higgs doublets with opposite hypercharge. Similarly Q , U , and D represent chiral multiplets of quarks of an $SU(2)_L$ doublet and two singlets with different $U(1)_Y$ charges. Three generations of leptons and quarks are assumed and thus the subscripts i and j run over 1 – 3. The symbol $\epsilon_{\alpha\beta}$ is an antisymmetric tensor with $\epsilon_{12} = 1$. The Yukawa interactions are derived from the superpotential via

$$\mathcal{L} = + \frac{1}{2} \sum_{i,j} \frac{\partial^2 W}{\partial \phi_i \partial \phi_j} \psi_i \psi_j + \text{H.c.} \quad (2)$$

SUSY is softly broken in our model. The general soft SUSY-breaking terms are given as

$$\begin{aligned} -\mathcal{L}_{\text{soft}} = & (m_{\tilde{Q}}^2)_i^j \tilde{q}_L^i \tilde{q}_L^j + (m_{\tilde{u}}^2)_j^i \tilde{u}_{Ri}^* \tilde{u}_R^j + (m_{\tilde{d}}^2)_j^i \tilde{d}_{Ri}^* \tilde{d}_R^j + (m_{\tilde{L}}^2)_i^j \tilde{l}_L^i \tilde{l}_L^j + (m_{\tilde{e}}^2)_j^i \tilde{e}_{Ri}^* \tilde{e}_R^j + (m_{\tilde{\nu}}^2)_j^i \tilde{\nu}_{Ri}^* \tilde{\nu}_R^j + \tilde{m}_{h_1}^2 h_1^\dagger h_1 + \tilde{m}_{h_2}^2 h_2^\dagger h_2 \\ & + (B\mu h_1 h_2 + \frac{1}{2} B_\nu^{ij} M_\nu^{ij} \tilde{\nu}_{Ri}^* \tilde{\nu}_R^j + \text{H.c.}) + (A_d^{ij} h_1 \tilde{d}_{Ri}^* \tilde{q}_L^j + A_u^{ij} h_2 \tilde{u}_{Ri}^* \tilde{q}_L^j + A_l^{ij} h_1 \tilde{e}_{Ri}^* \tilde{l}_L^j + A_\nu^{ij} h_2 \tilde{\nu}_{Ri}^* \tilde{l}_L^j + \frac{1}{2} M_1 \tilde{B}_L^0 \tilde{B}_L^0 \\ & + \frac{1}{2} M_2 \tilde{W}_L^a \tilde{W}_L^a + \frac{1}{2} M_3 \tilde{G}^a \tilde{G}^a + \text{H.c.}). \end{aligned} \quad (3)$$

Here the first eight terms are soft terms for sleptons, squarks, and Higgs bosons, while the terms with $M_1 - M_3$ give gaugino mass terms.

We now discuss LFV in the Yukawa couplings. Suppose that the Yukawa coupling matrix f_l^{ij} and the mass matrix of the right-handed neutrinos M_ν^{ij} are diagonalized as $f_{li} \delta^{ij}$ and $M_{Ri} \delta^{ij}$, respectively.¹ Then, in this basis, the neutrino Yukawa couplings f_ν^{ij} are not generally diagonal, giving rise to LFV. An immediate consequence is neutrino oscillation. Writing $f_\nu^{ij} = U^{ik} f_{\nu k} V^{kj}$ with U , V unitary matrices, we obtain the neutrino mass matrix induced by the seesaw mechanism:

$$m_\nu = f_\nu^T M_\nu^{-1} f_\nu \frac{v^2}{2} \sin^2 \beta = V^T \begin{pmatrix} f_{\nu 1} & & \\ & f_{\nu 2} & \\ & & f_{\nu 3} \end{pmatrix} U^T \begin{pmatrix} \frac{1}{M_{R1}} & & \\ & \frac{1}{M_{R2}} & \\ & & \frac{1}{M_{R3}} \end{pmatrix} U \begin{pmatrix} f_{\nu 1} & & \\ & f_{\nu 2} & \\ & & f_{\nu 3} \end{pmatrix} V \frac{v^2}{2} \sin^2 \beta, \quad (4)$$

where $\frac{1}{2} v^2 = \langle h_1 \rangle^2 + \langle h_2 \rangle^2 \simeq (174 \text{ GeV})^2$ and $\tan \beta = \langle h_2 \rangle / \langle h_1 \rangle$. (Here, the angular brackets stand for the vacuum expectation value of the quantity.) Throughout this paper, we assume that M_ν is proportional to the unit matrix $M_\nu^{ij} = M_R \delta^{ij}$, for simplicity. Then, if we disregard possible complex phases in U , the above can be rewritten as

$$m_\nu = \frac{1}{M_R} V^T \begin{pmatrix} f_{\nu 1}^2 & & \\ & f_{\nu 2}^2 & \\ & & f_{\nu 3}^2 \end{pmatrix} V \frac{v^2}{2} \sin^2 \beta. \quad (5)$$

Thus as far as $V \neq 1$ and the mass eigenvalues are non-degenerate, we have neutrino oscillation which is a target of current and future experiments.

¹We can always choose f_l^{ij} , and M_ν^{ij} to be diagonal by using unitary transformations of L , E^c and N^c .

The smallness of the neutrino masses implies that the scale M_R is very high, $\sim 10^{12}$ GeV or even higher. In the standard model with right-handed neutrinos, the flavor-violating processes such as $\mu \rightarrow e \gamma$, $\tau \rightarrow \mu \gamma$, etc., whose rates are proportional to inverse powers of M_R , would be highly suppressed with such a large M_R scale, and hence those would never be seen experimentally.

However, if there exists SUSY broken at the electroweak scale, we may expect that the rates of these LFV processes will be much larger than the nonsupersymmetric case. The point is that the lepton-flavor conservation is not a consequence of standard-model gauge symmetry and renormalizability in the supersymmetric case, even in the absence of the right-handed neutrinos. Indeed, slepton mass terms can violate the lepton-flavor conservation in a manner consistent with the gauge symmetry. Thus the scale of LFV can be identified with the electroweak scale, much lower than the right-handed neutrino scale M_R . However, an order-of-unity violation of lepton-flavor conservation at the electroweak scale would cause disastrously large rates for $\mu \rightarrow e \gamma$ and

others. Also, arbitrary squark masses result in too large rates for various flavor-changing-neutral-current processes involving squark loops. To avoid these problems, one often considers that sleptons and squarks are degenerate in masses among those with the same gauge quantum numbers in the tree-level Lagrangian at a certain renormalization scale. In the following, we will assume a somewhat stronger hypothesis that all SUSY-breaking scalar masses are universal at the gravitational scale $M \equiv m_{\text{Pl}}/\sqrt{8\pi} \sim 2 \times 10^{18}$ GeV; i.e., we adopt minimal-supergravity-type boundary conditions. Thus we will consider the following type of soft terms: universal scalar mass (m_0), all scalar masses of the type $(m_{\tilde{f}}^2)_i^j$ and $\tilde{m}_{h_i}^2$ ($i=1,2$) take common value m_0^2 , universal A parameter, $A_f^{ij} = a f_f^{ij} m_0$ with a being a constant of order unity, at the renormalization scale M .² As for the gaugino masses, for simplicity, we choose the boundary conditions so that they satisfy the so-called grand unified theory (GUT) relation at low energies. Note that the universal scalar masses are given in a certain class of supergravity models with hidden sector SUSY breaking [5]. Those soft SUSY breaking terms suffer from renormalization via gauge and Yukawa interactions, which can be conveniently expressed in terms of renormalization-group equations (RGE's). The RGE's relevant to our analysis will be given in Appendix A. An important point is that, through this renormalization effect, LFV in the Yukawa couplings induces LFV in the slepton masses at low energies even if the scalar masses are universal at high energy. Because of this fact, lepton-flavor conservation is violated at low energies.

We can solve the RGE's numerically with the boundary conditions given above. It is, however, instructive to consider here a simple approximation to estimate the LFV contribution to the slepton masses. Since the $SU(2)_L$ doublet lepton multiplets have the lepton-flavor-violating Yukawa couplings with the right-handed neutrino multiplets, the LFV effect most directly appears in the mass matrix of the doublet sleptons. The RGE's for them can be written as (see Appendix A)

$$\begin{aligned} \mu \frac{d}{d\mu} (m_{\tilde{L}}^2)_i^j = & \left(\mu \frac{d}{d\mu} (m_{\tilde{L}}^2)_i^j \right)_{\text{MSSM}} + \frac{1}{16\pi^2} [(m_{\tilde{L}}^2 f_{\nu}^\dagger f_\nu \\ & + f_{\nu}^\dagger f_\nu m_{\tilde{L}}^2)_i^j + 2(f_{\nu}^\dagger m_{\tilde{W}}^2 f_\nu + \tilde{m}_{h_2}^2 f_{\nu}^\dagger f_\nu + A_{\nu}^\dagger A_{\nu})_i^j]. \end{aligned} \quad (6)$$

Here $(\mu d/d\mu (m_{\tilde{L}}^2)_i^j)_{\text{MSSM}}$ denotes the RGE in case of the MSSM, and the terms explicitly written are additional contributions by the right-handed neutrino Yukawa couplings. An iteration gives an approximate solution for the additional contributions to the mass terms:

²In fact, there is another SUSY-breaking parameter B , which gives a mixing term of the two Higgs bosons h_1 and h_2 . For a given value of $\tan\beta$, we fix this parameter B (and also the SUSY invariant Higgs boson mass μ) so that the Higgs bosons have correct vacuum expectation values, $\langle h_1 \rangle = v \cos\beta/\sqrt{2}$ and $\langle h_2 \rangle = v \sin\beta/\sqrt{2}$.

$$\begin{aligned} (\Delta m_{\tilde{L}}^2)_i^j & \approx - \frac{\ln(M/M_R)}{16\pi^2} [6m_0^2 (f_{\nu}^\dagger f_\nu)_i^j + 2(A_{\nu}^\dagger A_{\nu})_i^j] \\ & = - \frac{\ln(M/M_R)}{16\pi^2} (6 + 2a^2) m_0^2 (f_{\nu}^\dagger f_\nu)_i^j, \end{aligned} \quad (7)$$

where we have used the universal scalar mass and A -parameter conditions. In Eq. (7),

$$(f_{\nu}^\dagger f_\nu)_i^j = f_{\nu ik}^\dagger f_{\nu}^{kj} = V_{ki}^* |f_{\nu k}|^2 V^{kj}, \quad (8)$$

so that the slepton mass $(m_{\tilde{L}}^2)_i^j$ indeed has generation mixing if V differs from the unit matrix in the basis that the charged lepton Yukawa couplings f_l are diagonal.

Lack of knowledge of the neutrino Yukawa couplings prevents us from giving a definite prediction of the slepton mass matrix, and thus the rates of the LFV processes. Nevertheless, it is important to study how large the interaction rates for the LFV processes can be for some typical cases and to see whether those signals can be tested by experiments. In this paper, we shall consider the following typical two cases: case (1), the mixing matrix V is identical to the Kobayashi-Maskawa (KM) matrix in the quark sector V_{KM} , and case (2), the mixing matrix is given so that it can explain atmospheric neutrino deficit by the large-mixing $\nu_\tau - \nu_\mu$ oscillation. In the latter case, we only consider $\tau \rightarrow \mu \gamma$, the generation mixing between the second and third ones.

III. INTERACTION RATES FOR LFV PROCESSES

In this section we give formulas of the interaction rates for the LFV processes we consider. The results of our numerical calculation will be given in the next section.

We first explain how the rates for $\mu \rightarrow e \gamma$ and $\tau \rightarrow \mu \gamma$ can be enhanced compared with the naive expectation when $\tan\beta$ is large. Here, we consider in the basis where the neutralino or chargino interactions to the leptons and the sleptons are flavor diagonal and the effect of flavor violation in the lepton sector is involved by the mass insertions $(m_{\tilde{L}}^2)_i^j$ ($i \neq j$). First, let us consider contribution from W -inos and B -inos, the $SU(2)_L \times U(1)_Y$ gauginos, neglecting the mixing in the chargino or neutralino sector. A naive estimate on the branching ratio yields

$$B(l_j \rightarrow l_i \gamma) \propto \frac{\alpha^3}{G_F^2} \frac{[(m_{\tilde{L}}^2)_i^j]^2}{m_S^8}, \quad (9)$$

where m_S is the typical mass of superparticles, α the fine structure constant, and G_F the Fermi constant. The contribution from the Feynman diagrams, Figs. 1(a) and 1(b), follows this estimate. However, as emphasized in our previous paper [3], the diagram of Fig. 1(c) which picks up the left-right mixing of the sleptons and exchanges the B -ino in the loop can give a much larger contribution when $\mu \tan\beta$ is much larger than the masses of the other superparticles. Indeed we estimate the ratio of the amplitudes

$$\frac{\text{Amp}[1(c)]}{\text{Amp}[1(a) + 1(b)]} \sim \frac{M_1 m_{LRjj}^2}{m_l m_S^2} \sim \frac{\mu \tan\beta}{m_S} \frac{M_1}{m_S}, \quad (10)$$

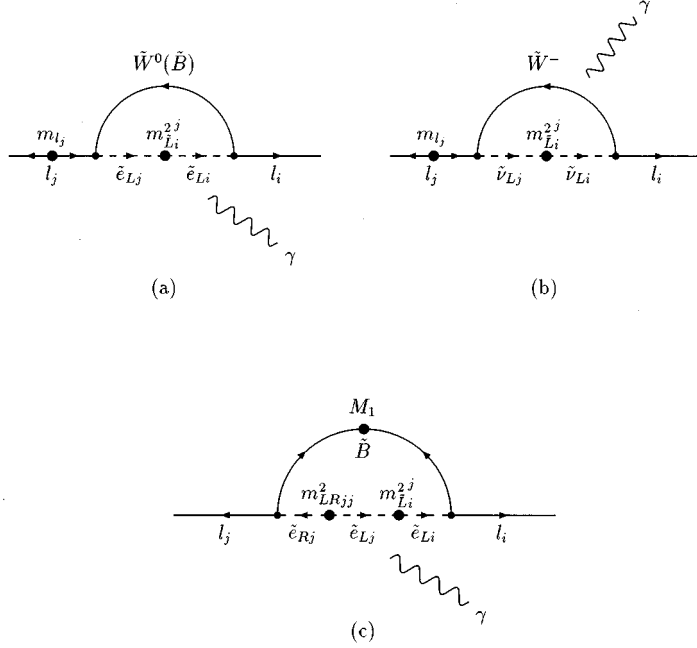


FIG. 1. Feynman diagrams which give rise to $l_j \rightarrow l_i \gamma$. The symbols \tilde{e}_{Li} , $\tilde{\nu}_{Li}$, \tilde{B} , \tilde{W}^0 , and \tilde{W}^- represent left-handed charged sleptons, left-handed sneutrinos, B -ino, neutral W -ino, and charged W -ino, respectively. In (a) and (b), the blob in the the slepton or sneutrino line indicates the flavor-violating mass insertion of the left-handed slepton and another blob in the external line the chirality flip of the external lepton l_j . In (c), the blobs in the slepton line indicate the insertions of the flavor-violating mass (m_{Li}^{2j}) and the left-right mixing mass (m_{LRjj}^2), and another blob in the B -ino line the chirality flip of the B -ino \tilde{B} .

with m_{l_j} being the charged lepton l_j mass. In Ref. [3], we numerically showed that this enhancement really occurs for the case of large $\mu \tan \beta$.

If we take account of the gaugino-Higgsino mixing in the chargino or neutralino sector, we find another type of diagram which enhances the amplitude when $\tan \beta$ is large but μ is comparable to the masses of the other superparticles. It is shown in Fig. 2. In this diagram, one has mixing between the Higgsino and the gaugino which is proportional to $v \sin \beta$, the vacuum expectation value of h_2 , and involves the Yukawa coupling of Higgsinos, leptons, and sleptons, $f_{l_j} = -\sqrt{2} m_{l_j} / (v \cos \beta)$. The sleptons inside a loop are left-handed ones. Thus the amplitude is proportional to $\tan \beta$, and

$$\frac{\text{Amp}(2)}{\text{Amp}[1(a)+1(b)]} \sim \tan \beta. \quad (11)$$

Note that this type of diagram includes neutralino-exchange graphs as well as a chargino-exchange graph.

In this work, we are interested in the LFV processes $\mu \rightarrow e \gamma$ and $\tau \rightarrow \mu \gamma$, $\mu^- \rightarrow e^- e^- e^+$, and μ - e conversion in nuclei. To obtain the interaction rates for these processes, we perform a full diagonalization of the slepton mass matrices numerically and consider mixing in the chargino and neutralino sectors.

We write the interaction Lagrangian of fermions, sfermions, and neutralinos as

$$\mathcal{L} = \bar{f}_i (N_{iAX}^{R(f)} P_R + N_{iAX}^{L(f)} P_L) \tilde{\chi}_A^0 \tilde{f}_X + \text{H.c.} \quad (12)$$

In this section, f_i ($f=l, \nu, d, u$) represents a fermion in a mass eigenstate with the generation index i ($i=1,2,3$), and \tilde{f}_X a sfermion in a mass eigenstate. The subscript X runs from 1 to 3 for $\tilde{\nu}$ and from 1 to 6 for the other sfermions, \tilde{l}, \tilde{d} , and \tilde{u} . A neutralino mass eigenstate is denoted by $\tilde{\chi}_A^0$ ($A=1, \dots, 4$) and $P_{R,L} = \frac{1}{2}(1 \pm \gamma_5)$. The coefficients $N_{iAX}^{R(f)}$ and $N_{iAX}^{L(f)}$ depend on the mixing matrices of the neutralino

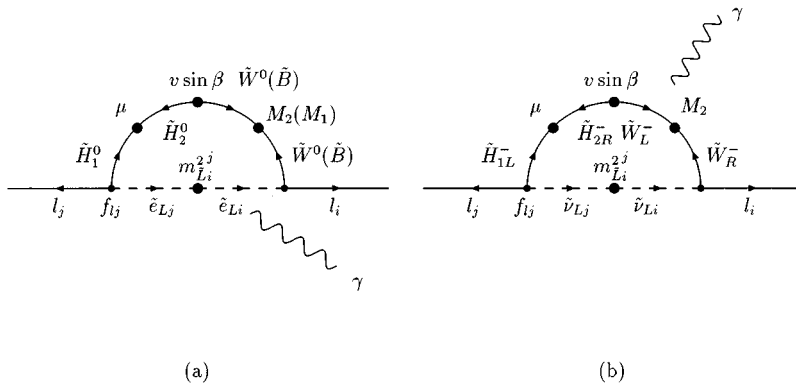


FIG. 2. Feynman diagrams which give rise to the large $\tan \beta$ enhancement due to the gaugino-Higgsino mixing in the process of $l_j \rightarrow l_i \gamma$. The symbols \tilde{e}_{Li} , $\tilde{\nu}_{Li}$, \tilde{B} , \tilde{W}^0 , \tilde{W}^- , \tilde{H}^0 , and \tilde{H}^- represent left-handed charged sleptons, left-handed sneutrinos, B -ino, neutral W -ino, charged W -ino, neutral Higgsino, and charged Higgsino, respectively. The blob in the slepton or sneutrino line indicates the insertion of the flavor-violating mass (m_{Li}^{2j}). The blobs in the gaugino-Higgsino line indicate the mass insertions for gaugino-Higgsino mixing; that is, μ denotes Higgsino (\tilde{H}_1 - \tilde{H}_2) mass mixing, $v \sin \beta$ the gaugino-Higgsino (\tilde{H}_2 - \tilde{W}) mass mixing, and M_2 the W -ino mass. The value of $\tan \beta$ comes from the Yukawa coupling constant $f_{l_j} \sim 1/\cos \beta$ and vacuum expectation value (VEV) of h_2 , $v \sin \beta$.

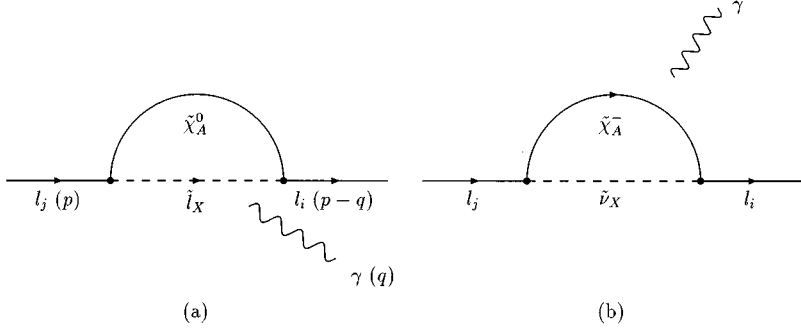


FIG. 3. Feynman diagrams for the process $l_j \rightarrow l_i \gamma$. (a) represents the contributions from neutralino $\tilde{\chi}_A^0$ and slepton \tilde{l}_X loops, and (b) the contributions from chargino $\tilde{\chi}_A^-$ and sneutrino $\tilde{\nu}_X$ loops.

sector and of the sfermions. Their explicit forms will be given in Appendix B. Similarly the fermion-sfermion-chargino interaction is written as

$$\begin{aligned} \mathcal{L} = & \bar{l}_i (C_{iAX}^{R(l)} P_R + C_{iAX}^{L(l)} P_L) \tilde{\chi}_A^- \tilde{\nu}_X + \bar{\nu}_i (C_{iAX}^{R(v)} P_R \\ & + C_{iAX}^{L(v)} P_L) \tilde{\chi}_A^+ \tilde{l}_X + \bar{d}_i (C_{iAX}^{R(d)} P_R + C_{iAX}^{L(d)} P_L) \tilde{\chi}_A^- \tilde{u}_X \\ & + \bar{u}_i (C_{iAX}^{R(u)} P_R + C_{iAX}^{L(u)} P_L) \tilde{\chi}_A^+ \tilde{d}_X + \text{H.c.}, \end{aligned} \quad (13)$$

where $\tilde{\chi}_A^\pm$ ($A=1,2$) is a chargino mass eigenstate. The explicit forms of the coefficients can also be found in Appendix B.

A. Effective Lagrangian for LFV processes

As a first step to compute the LFV rates, let us write down the effective interactions (or amplitudes) relevant for our purpose.

$$I. l_j^- \rightarrow l_i^- \gamma^*$$

The off-shell amplitude for $l_j^- \rightarrow l_i^- \gamma^*$ is generally written as

$$\begin{aligned} T = & e \epsilon^{\alpha*} \bar{u}_i(p-q) [q^2 \gamma_\alpha (A_1^L P_L + A_1^R P_R) \\ & + m_{l_j} i \sigma_{\alpha\beta} q^\beta (A_2^L P_L + A_2^R P_R)] u_j(p), \end{aligned} \quad (14)$$

in the limit of $q \rightarrow 0$ with q being the photon momentum. Here, e is the electric charge, ϵ^* the photon polarization vector, u_i (and v_i in the expressions below) the wave function for (anti) lepton, and p the momentum of the particle l_j . In the present case, the Feynman diagrams contributing to the above amplitude are depicted by Fig. 3. Each coefficient in the above can be written as a sum of two terms,

$$A_a^{L,R} = A_a^{(n)L,R} + A_a^{(c)L,R} \quad (a=1,2),$$

where $A_a^{(n)L,R}$ and $A_a^{(c)L,R}$ stand for the contributions from the neutralino loops and from the chargino loops, respectively. We calculate them and find that the neutralino contributions are given by

$$A_1^{(n)L} = \frac{1}{576\pi^2} N_{iAX}^{R(l)} N_{jAX}^{R(l)*} \frac{1}{m_{\tilde{l}_X}^2} \frac{1}{(1-x_{AX})^4} (2 - 9x_{AX} + 18x_{AX}^2 - 11x_{AX}^3 + 6x_{AX}^3 \ln x_{AX}), \quad (15)$$

$$\begin{aligned} A_2^{(n)L} = & \frac{1}{32\pi^2} \frac{1}{m_{\tilde{l}_X}^2} \left[N_{iAX}^{L(l)} N_{jAX}^{L(l)*} \frac{1}{6(1-x_{AX})^4} (1 - 6x_{AX} + 3x_{AX}^2 + 2x_{AX}^3 - 6x_{AX}^2 \ln x_{AX}) \right. \\ & \left. + N_{iAX}^{L(l)} N_{jAX}^{R(l)*} \frac{M_{\tilde{\chi}_A^0}}{m_{l_j}} \frac{1}{(1-x_{AX})^3} (1 - x_{AX}^2 + 2x_{AX} \ln x_{AX}) \right], \end{aligned} \quad (16)$$

$$A_a^{(n)R} = A_a^{(n)L} |_{L \leftrightarrow R} \quad (a=1,2), \quad (17)$$

where $x_{AX} = M_{\tilde{\chi}_A^0}^2 / m_{\tilde{l}_X}^2$ is the ratio of the neutralino mass squared $M_{\tilde{\chi}_A^0}^2$, to the charged slepton mass squared $m_{\tilde{l}_X}^2$. (A summation over the indices A and X is assumed to be understood.) The chargino contributions are

$$A_1^{(c)L} = - \frac{1}{576\pi^2} C_{iAX}^{R(l)} C_{jAX}^{R(l)*} \frac{1}{m_{\tilde{\nu}_X}^2} \frac{1}{(1-x_{AX})^4} \{16 - 45x_{AX} + 36x_{AX}^2 - 7x_{AX}^3 + 6(2 - 3x_{AX}) \ln x_{AX}\}, \quad (18)$$

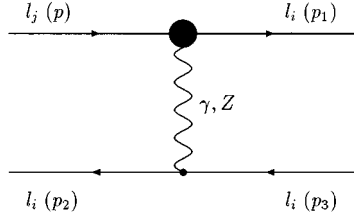


FIG. 4. Penguin-type diagrams for the process $l_j^- \rightarrow l_i^- l_i^- l_i^+$ in which a photon γ and Z boson are exchanged. The blob indicates an $l_j^- l_i^- \gamma$ vertex such as Fig. 3 or an $l_j^- l_i^- Z$ vertex where the Z boson is external.

$$A_2^{(c)L} = -\frac{1}{32\pi^2} \frac{1}{m_{\tilde{\nu}_X}^2} \left[C_{iAX}^{L(l)} C_{jAX}^{L(l)*} \frac{1}{6(1-x_{AX})^4} (2+3x_{AX}-6x_{AX}^2+x_{AX}^3+6x_{AX}\ln x_{AX}) \right. \\ \left. + C_{iAX}^{L(l)} C_{jAX}^{R(l)*} \frac{M_{\tilde{\chi}_A^-}}{m_{l_j}} \frac{1}{(1-x_{AX})^3} (-3+4x_{AX}-x_{AX}^2-2\ln x_{AX}) \right], \quad (19)$$

$$A_a^{(c)R} = A_a^{(c)L}|_{L \leftrightarrow R} \quad (a=1,2). \quad (20)$$

Here, $x_{AX} = M_{\tilde{\chi}_A^-}^2/m_{\tilde{\nu}_X}^2$, where $M_{\tilde{\chi}_A^-}$ and $m_{\tilde{\nu}_X}$ are the masses for the chargino $\tilde{\chi}_A^-$ and the sneutrino $\tilde{\nu}_X$, respectively.

2. $l_j^- \rightarrow l_i^- l_i^- l_i^+$

We next consider the process $l_j^- \rightarrow l_i^- l_i^- l_i^+$ (including $\mu^- \rightarrow e^- e^- e^+$). The effective amplitude consists of the contributions from penguin-type diagrams and from box-type diagrams. The former contribution can be computed using Eq. (14), with the result

$$T_{\gamma\text{-penguin}} = \bar{u}_i(p_1) [q^2 \gamma_\alpha (A_1^L P_L + A_1^R P_R) + m_{l_j} i \sigma_{\alpha\beta} q^\beta (A_2^L P_L + A_2^R P_R)] u_j(p) \frac{e^2}{q^2} \bar{u}_i(p_2) \gamma^\alpha v_i(p_3) - (p_1 \leftrightarrow p_2). \quad (21)$$

Furthermore, there are the other penguin-type diagrams in which the Z boson is exchanged as shown in Fig. 4. This amplitude is

$$T_{Z\text{-penguin}} = \frac{g_Z^2}{m_Z^2} \bar{u}_i(p_1) \gamma^\mu (F_L P_L + F_R P_R) u_j(p) \bar{u}_i(p_2) \gamma^\mu (Z_L^L P_L + Z_R^L P_R) v_i(p_3) - (p_1 \leftrightarrow p_2), \quad (22)$$

where $F_{L(R)} = F_{L(R)}^{(c)} + F_{L(R)}^{(n)}$. The chargino contribution $F_{L(R)}^{(c)}$ and the neutralino contribution $F_{L(R)}^{(n)}$ are³

$$F_L^{(c)} = -\frac{C_{iAX}^{R(l)} C_{jBX}^{R(l)*}}{16\pi^2} \left[\frac{(O_R)_{A2} (O_R)_{B2}}{4} F_{(X,A,B)} - \frac{(O_L)_{A2} (O_L)_{B2}}{2} G_{(X,A,B)} \right], \quad (23)$$

$$F_R^{(c)} = 0, \quad (24)$$

$$F_L^{(n)} = \frac{N_{iAX}^{R(l)} N_{jBX}^{R(l)*}}{16\pi^2} \frac{(O_N)_{A3} (O_N)_{B3} - (O_N)_{A4} (O_N)_{B4}}{2} (F_{(X,A,B)} + 2G_{(X,A,B)}), \quad (25)$$

$$F_R^{(n)} = -F_L^{(n)}|_{L \leftrightarrow R}. \quad (26)$$

Here, $O_{L,R}$ and O_N are orthogonal matrices to diagonalize the mass matrices of the chargino and neutralino (see Appendix B), and $F_{(X,A,B)}$ and $G_{(X,A,B)}$ are given by

$$F_{(X,A,B)} = \ln x_{AX} + \frac{1}{x_{AX} - x_{BX}} \left(\frac{x_{AX}^2 \ln x_{AX}}{1 - x_{AX}} - \frac{x_{BX}^2 \ln x_{BX}}{1 - x_{BX}} \right), \quad (27)$$

³The penguin-type diagrams of the Z boson contributing to the LFV events do not necessarily need to have a chirality flip of leptons as $\mu \rightarrow e \gamma$. Therefore, the diagrams picking up the Yukawa coupling of Higgsinos, fermions, and sfermions cannot become the dominant contribution in Z-boson penguin-type diagrams and we neglect them in the above equations.

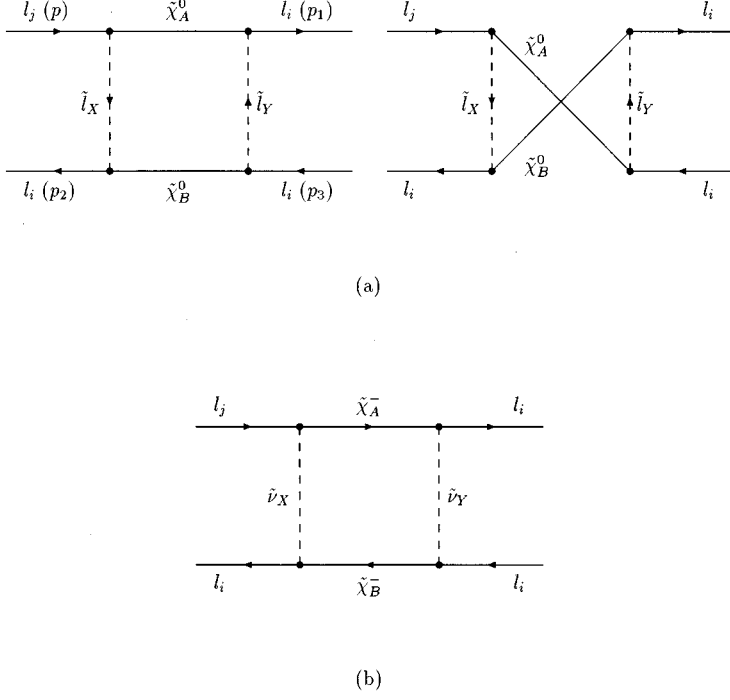


FIG. 5. Box-type diagrams for the process $l_j^- \rightarrow l_i^- l_i^- l_i^+$. Here, (a) represents the contributions from neutralino $\tilde{\chi}_A^0$ and slepton \tilde{l}_X loops, while (b) the contributions from chargino $\tilde{\chi}_A^-$ and sneutrino $\tilde{\nu}_X$ loops.

$$G_{(X,A,B)} = \frac{M_{\tilde{\chi}_A} M_{\tilde{\chi}_B}}{m_{\tilde{l}_X}^2} \frac{1}{x_{AX} - x_{BX}} \left(\frac{x_{AX} \ln x_{AX}}{1 - x_{AX}} - \frac{x_{BX} \ln x_{BX}}{1 - x_{BX}} \right). \quad (28)$$

In these functions, $M_{\tilde{\chi}_A}$ and $m_{\tilde{l}_X}$ denote neutralino mass and charged slepton mass in the neutralino contribution, and chargino mass and sneutrino mass in the chargino contribution. And in Eq. (22) the coefficient $Z_{L(R)}^l$ denotes Z boson coupling to charged lepton $l_{L(R)}$: that is,

$$Z_{L(R)}^l = T_{3L(R)}^l - Q_{\text{em}}^l \sin^2 \theta_W, \quad (29)$$

where $T_{3L(R)}^l$ and Q_{em}^l represent weak isospin ($T_{3L}^l = -\frac{1}{2}$, $T_{3R}^l = 0$) and electric charge ($Q_{\text{em}}^l = -1$) of $l_{L(R)}$, respectively.

The box-type Feynman diagrams are given in Fig. 5, and we can write their amplitude as

$$\begin{aligned} T_{\text{box}} = & B_1^L e^2 \bar{u}_i(p_1) \gamma^\alpha P_L u_j(p) \bar{u}_i(p_2) \gamma_\alpha P_L v_i(p_3) + B_1^R e^2 \bar{u}_i(p_1) \gamma^\alpha P_R u_j(p) \bar{u}_i(p_2) \gamma_\alpha P_R v_i(p_3) \\ & + B_2^L e^2 \{ \bar{u}_i(p_1) \gamma^\alpha P_L u_j(p) \bar{u}_i(p_2) \gamma_\alpha P_R v_i(p_3) - (p_1 \leftrightarrow p_2) \} + B_2^R e^2 \{ \bar{u}_i(p_1) \gamma^\alpha P_R u_j(p) \bar{u}_i(p_2) \gamma_\alpha P_L v_i(p_3) - (p_1 \leftrightarrow p_2) \} \\ & + B_3^L e^2 \{ \bar{u}_i(p_1) P_L u_j(p) \bar{u}_i(p_2) P_L v_i(p_3) - (p_1 \leftrightarrow p_2) \} + B_3^R e^2 \{ \bar{u}_i(p_1) P_R u_j(p) \bar{u}_i(p_2) P_R v_i(p_3) - (p_1 \leftrightarrow p_2) \} \\ & + B_4^L e^2 \{ \bar{u}_i(p_1) \sigma_{\mu\nu} P_L u_j(p) \bar{u}_i(p_2) \sigma^{\mu\nu} P_L v_i(p_3) - (p_1 \leftrightarrow p_2) \} + B_4^R e^2 \{ \bar{u}_i(p_1) \sigma_{\mu\nu} P_R u_j(p) \bar{u}_i(p_2) \sigma^{\mu\nu} P_R v_i(p_3) \\ & - (p_1 \leftrightarrow p_2) \}, \end{aligned} \quad (30)$$

where

$$B_a^{L,R} = B_a^{(n)L,R} + B_a^{(c)L,R} \quad (a = 1, \dots, 4). \quad (31)$$

The first term represents the neutralino contribution, which we find to be

$$e^2 B_1^{(n)L} = \frac{1}{2} J_{4(A,B,X,Y)} N_{jAX}^{R(l)*} N_{iAY}^{R(l)} N_{iBY}^{R(l)*} N_{iBX}^{R(l)} + I_{4(A,B,X,Y)} M_{\tilde{\chi}_A^0} M_{\tilde{\chi}_B^0} N_{jAX}^{R(l)*} N_{iAY}^{R(l)} N_{iBY}^{R(l)*} N_{iBX}^{R(l)}, \quad (32)$$

$$\begin{aligned} e^2 B_2^{(n)L} = & \frac{1}{4} J_{4(A,B,X,Y)} \{ N_{jAX}^{R(l)*} N_{iAY}^{R(l)} N_{iBY}^{L(l)*} N_{iBX}^{L(l)} + N_{jAX}^{R(l)*} N_{iAY}^{L(l)*} N_{iBY}^{R(l)} N_{iBX}^{L(l)} - N_{jAX}^{R(l)*} N_{iAY}^{L(l)*} N_{iBY}^{L(l)*} N_{iBX}^{R(l)} \} \\ & - \frac{1}{2} I_{4(A,B,X,Y)} M_{\tilde{\chi}_A^0} M_{\tilde{\chi}_B^0} N_{jAX}^{R(l)*} N_{iAY}^{L(l)} N_{iBY}^{L(l)*} N_{iBX}^{R(l)}, \end{aligned} \quad (33)$$

$$e^2 B_3^{(n)L} = I_{4(A,B,X,Y)} M_{\tilde{\chi}_A^0} M_{\tilde{\chi}_B^0} \left\{ N_{jAX}^{R(l)*} N_{iAY}^{L(l)} N_{iBY}^{R(l)*} N_{iBX}^{L(l)} + \frac{1}{2} N_{jAX}^{R(l)*} N_{iAY}^{R(l)*} N_{iBY}^{L(l)} N_{iBX}^{L(l)} \right\}, \quad (34)$$

$$e^2 B_4^{(n)L} = \frac{1}{8} I_{4(A,B,X,Y)} M_{\tilde{\chi}_A^0} M_{\tilde{\chi}_B^0} N_{jAX}^{R(l)*} N_{iAY}^{R(l)*} N_{iBY}^{L(l)} N_{iBX}^{L(l)}, \quad (35)$$

$$B_a^{(n)R} = B_a^{(n)L} |_{L \leftrightarrow R} \quad (a=1, \dots, 4). \quad (36)$$

The chargino contribution is

$$e^2 B_1^{(c)L} = \frac{1}{2} J_{4(A,B,X,Y)} C_{jAX}^{R(l)*} C_{iAY}^{R(l)} C_{iBY}^{R(l)*} C_{iBX}^{R(l)}, \quad (37)$$

$$e^2 B_2^{(c)L} = \frac{1}{4} J_{4(A,B,X,Y)} C_{jAX}^{R(l)*} C_{iAY}^{R(l)} C_{iBY}^{L(l)*} C_{iBX}^{L(l)} - \frac{1}{2} I_{4(A,B,X,Y)} M_{\tilde{\chi}_A^-} M_{\tilde{\chi}_B^-} C_{jAX}^{R(l)*} C_{iAY}^{L(l)} C_{iBY}^{L(l)*} C_{iBX}^{R(l)}, \quad (38)$$

$$e^2 B_3^{(c)L} = I_{4(A,B,X,Y)} M_{\tilde{\chi}_A^-} M_{\tilde{\chi}_B^-} C_{jAX}^{R(l)*} C_{iAY}^{L(l)} C_{iBY}^{R(l)*} C_{iBX}^{L(l)}, \quad (39)$$

$$B_4^{(c)L} = 0, \quad (40)$$

$$B_a^{(c)R} = B_a^{(c)L} |_{L \leftrightarrow R} \quad (a=1, \dots, 4), \quad (41)$$

where

$$iJ_{4(A,B,X,Y)} = \int \frac{d^4 k}{(2\pi)^4} \frac{k^2}{(k^2 - M_{\tilde{\chi}_A^0}^2)(k^2 - M_{\tilde{\chi}_B^0}^2)(k^2 - m_{\tilde{l}_X^+}^2)(k^2 - m_{\tilde{l}_Y^+}^2)}, \quad (42)$$

$$iI_{4(A,B,X,Y)} = \int \frac{d^4 k}{(2\pi)^4} \frac{1}{(k^2 - M_{\tilde{\chi}_A^0}^2)(k^2 - M_{\tilde{\chi}_B^0}^2)(k^2 - m_{\tilde{l}_X^+}^2)(k^2 - m_{\tilde{l}_Y^+}^2)}. \quad (43)$$

Here, $M_{\tilde{\chi}_A}$ and $m_{\tilde{l}_X}$ denote neutralino mass and charged slepton mass in the neutralino contribution, and chargino mass and sneutrino mass in the chargino contribution.

3. μ - e conversion in nuclei

Finally, we give the formulas for the μ - e conversion in nuclei, i.e., the process $[\mu + (A, Z) \rightarrow e + (A, Z)]$ where Z and A denote the proton and atomic numbers in a nucleus, respectively. The contribution again consists of penguin-type diagrams and box-type diagrams. The box-type Feynman diagrams are depicted in Figs. 6(b) and 6(c). We give the effective Lagrangian relevant to this process at the quark level. We find that the penguin-type diagrams give the terms

$$\begin{aligned} \mathcal{L}_{\text{eff}}^{\text{penguin}} = & -\frac{e^2}{q^2} \bar{e} [q^2 \gamma_\alpha (A_1^L P_L + A_1^R P_R) + m_\mu i \sigma_{\alpha\beta} q^\beta (A_2^L P_L \\ & + A_2^R P_R)] \mu \times \sum_{q=u,d} Q_{em}^q \bar{q} \gamma^\alpha q \\ & + \frac{g_Z^2}{m_{Zq}^2} \sum_{q=u,d} \frac{Z_L^q + Z_R^q}{2} \bar{q} \gamma_\alpha q \bar{e} \gamma^\alpha (F_L P_L + F_R P_R) \mu, \end{aligned} \quad (44)$$

where the first term comes from the penguin-type diagrams of photon exchange and the second one Z boson exchange.

The coefficient Q_{em}^q denotes the electric charge of the quark q and $Z_{L(R)}^q$ is the Z boson coupling to the quark $q_{L(R)}$ given by Eq. (29).

The box-type diagrams give

$$\mathcal{L}_{\text{eff}}^{\text{box}} = e^2 \sum_{q=u,d} \bar{q} \gamma_\alpha q \bar{e} \gamma^\alpha (D_q^L P_L + D_q^R P_R) \mu, \quad (45)$$

with

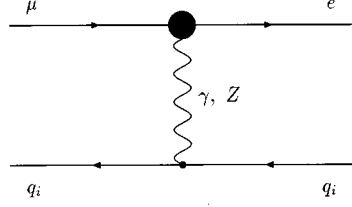
$$D_q^{L,R} = D_q^{(n)L,R} + D_q^{(c)L,R} \quad (q=u,d). \quad (46)$$

The coefficients are calculated to be

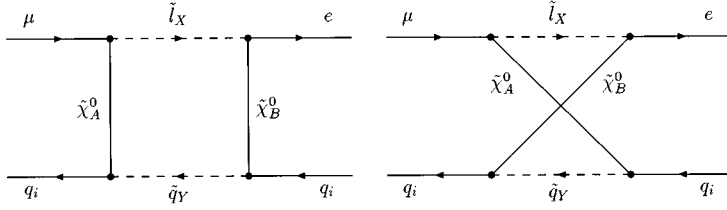
$$\begin{aligned} e^2 D_q^{(n)L} = & \frac{1}{8} J_{4(A,B,X,Y)} (N_{\mu AX}^{R(l)*} N_{e BX}^{R(l)} N_{q AY}^{R(q)} N_{q BY}^{R(q)*} \\ & - N_{\mu AX}^{R(l)*} N_{e BX}^{R(l)} N_{q AY}^{L(q)} N_{q BY}^{L(q)}) - \frac{1}{4} M_{\tilde{\chi}_A^0} M_{\tilde{\chi}_B^0} I_{4(A,B,X,Y)} \\ & \times (N_{\mu AX}^{R(l)*} N_{e BX}^{R(l)} N_{q AY}^{L(q)} N_{q BY}^{L(q)*} \\ & - N_{\mu AX}^{R(l)*} N_{e BX}^{R(l)} N_{q AY}^{R(q)} N_{q BY}^{R(q)*}), \end{aligned} \quad (47)$$

$$D_q^{(n)R} = D_q^{(n)L} |_{L \leftrightarrow R} \quad (q=u,d), \quad (48)$$

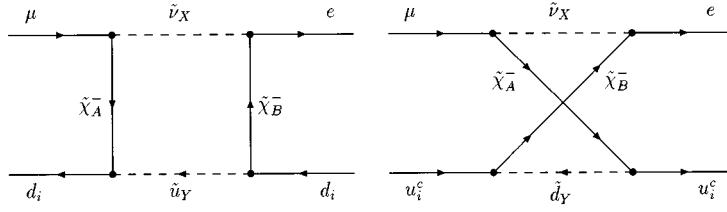
and



(a)



(b)



(c)

FIG. 6. Feynman diagrams for the μ - e conversion processes at the quark level. In (a), the penguin-type diagram is depicted. The blob indicates an l_j - l_i - γ vertex such as Fig. 3 or an l_j - l_i - Z vertex such as Fig. 4. In (b) and (c), the box-type diagrams are depicted; i.e., (b) represents the contributions from neutralino $\tilde{\chi}_A^0$, slepton \tilde{l}_X , and squark \tilde{q}_X ($q=u,d$) loops, and (c) the contributions from chargino $\tilde{\chi}_A^-$, sneutrino $\tilde{\nu}_X$, and squark \tilde{q}_X ($q=u,d$) loops.

$$e^2 D_d^{(c)L} = \frac{1}{8} J_{4(A,B,X,Y)} C_{\mu AX}^{R(l)*} C_{e BX}^{R(l)} C_{d AY}^{R(d)} C_{d BY}^{R(d)*} - \frac{1}{4} M_{\tilde{\chi}_A^-} M_{\tilde{\chi}_B^-} I_{4(A,B,X,Y)} C_{\mu AX}^{R(l)*} C_{e BX}^{R(l)} C_{d AY}^{L(d)} C_{d BY}^{L(d)*}, \quad (49)$$

$$e^2 D_u^{(c)L} = -\frac{1}{8} J_{4(A,B,X,Y)} C_{\mu AX}^{R(l)*} C_{e BX}^{R(l)} C_{u AY}^{L(u)*} C_{u BY}^{L(u)} + \frac{1}{4} M_{\tilde{\chi}_A^-} M_{\tilde{\chi}_B^-} I_{4(A,B,X,Y)} C_{\mu AX}^{R(l)*} C_{e BX}^{R(l)} C_{u AY}^{R(u)*} C_{u BY}^{R(u)}. \quad (50)$$

Note that we only take account of the vector contributions for the quark currents. The reason is given as follows. In the limit of low momentum transfer which is appropriate for the present case ($q^2 \simeq -m_\mu^2$), we can treat the hadronic current in the nonrelativistic limit. Furthermore, contributions from the coherent process dominate over incoherent ones if we concentrate on relevant processes such as $\mu + \frac{48}{22}\text{Ti}$

$\rightarrow e + \frac{48}{22}\text{Ti}$. Then, the matrix element for the μ - e conversion process is dominated by the contribution from the vector currents.

B. Decay rates and conversion rate

Now it is straightforward to calculate the decay rates and the conversion rate, using the amplitudes (or the effective Lagrangian) given in the above subsection.

1. $l_j^- \rightarrow l_i^- \gamma$ decay rate

The decay rate for $l_j^- \rightarrow l_i^- \gamma$ is easily calculated using the amplitude (14):

$$\Gamma(l_j^- \rightarrow l_i^- \gamma) = \frac{e^2}{16\pi} m_{l_j}^5 (|A_2^L|^2 + |A_2^R|^2). \quad (51)$$

2. $l_j^- \rightarrow l_i^- l_i^+ l_i^+$ decay rate

Using the expressions for the amplitude, we can calculate the decay rate:

$$\begin{aligned}
\Gamma(l_j^- \rightarrow l_i^- l_i^- l_i^+) &= \frac{e^4}{512\pi^3} m_{l_j}^5 \left[|A_1^L|^2 + |A_1^R|^2 - 2(A_1^L A_2^{R*} + A_2^L A_1^{R*} + \text{H.c.}) + (|A_2^L|^2 + |A_2^R|^2) \left(\frac{16}{3} \ln \frac{m_{l_j}}{2m_{l_i}} - \frac{14}{9} \right) \right. \\
&+ \frac{1}{6} (|B_1^L|^2 + |B_1^R|^2) + \frac{1}{3} (|B_2^L|^2 + |B_2^R|^2) + \frac{1}{24} (|B_3^L|^2 + |B_3^R|^2) + 6(|B_4^L|^2 + |B_4^R|^2) - \frac{1}{2} (B_3^L B_4^{L*} + B_3^R B_4^{R*} + \text{H.c.}) \\
&+ \frac{1}{3} (A_1^L B_1^{L*} + A_1^R B_1^{R*} + A_1^L B_2^{L*} + A_1^R B_2^{R*} + \text{H.c.}) - \frac{2}{3} (A_2^R B_1^{L*} + A_2^L B_1^{R*} + A_2^L B_2^{R*} + A_2^R B_2^{L*} + \text{H.c.}) \\
&+ \frac{1}{3} \{2(|F_{LL}|^2 + |F_{RR}|^2) + |F_{LR}|^2 + |F_{RL}|^2 + (B_1^L F_{LL}^* + B_1^R F_{RR}^* + B_2^L F_{LR}^* + B_2^R F_{RL}^* + \text{H.c.}) \\
&+ 2(A_1^L F_{LL}^* + A_1^R F_{RR}^* + \text{H.c.}) + (A_1^L F_{LR}^* + A_1^R F_{RL}^* + \text{H.c.}) - 4(A_2^R F_{LL}^* + A_2^L F_{RR}^* + \text{H.c.}) \\
&\left. - 2(A_2^L F_{RL}^* + A_2^R F_{LR}^* + \text{H.c.}) \right], \tag{52}
\end{aligned}$$

where

$$F_{LL} = \frac{F_L Z_L^L}{m_Z^2 \sin^2 \theta_W \cos^2 \theta_W}, \tag{53}$$

$$F_{RR} = F_{LL}|_{L \leftrightarrow R}, \tag{54}$$

$$F_{LR} = \frac{F_L Z_R^L}{m_Z^2 \sin^2 \theta_W \cos^2 \theta_W}, \tag{55}$$

$$F_{RL} = F_{LR}|_{L \leftrightarrow R}. \tag{56}$$

Numerically, we find that a penguin-type contribution involving A_2^L and A_2^R dominates over the other contributions. In the large $\tan\beta$ region, its effect is enhanced due to the same mechanism as in the case of the $l_j^- \rightarrow l_i^- \gamma$ process. Furthermore, even in the case where $\tan\beta$ is not so large, the contribution of the penguin-type diagram dominates over the box contribution, because of the logarithmic term in Eq. (52) which is quite larger than the other terms.⁴ Then, the above formula is greatly simplified, and one finds a simple relation

$$\frac{B(l_j^- \rightarrow l_i^- l_i^- l_i^+)}{B(l_j^- \rightarrow l_i^- \gamma)} \simeq \frac{\alpha}{8\pi} \left(\frac{16}{3} \ln \frac{m_{l_j}}{2m_{l_i}} - \frac{14}{9} \right). \tag{57}$$

3. μ - e conversion rate [$\mu + (A, Z) \rightarrow e + (A, Z)$]

Once we know the effective Lagrangian relevant to this process at the quark level, we can calculate the conversion rate [7]:

⁴This logarithmic term is obtained as a result of the phase space integration of the fermions in the final state, since we have an infrared singularity in the limit of $m_{l_i} \rightarrow 0$.

$$\begin{aligned}
\Gamma(\mu \rightarrow e) &= 4\alpha^5 \frac{Z_{\text{eff}}^4}{Z} |F(q)|^2 m_\mu^5 [|Z(A_1^L - A_2^R) - (2Z + N) \bar{D}_u^L| \\
&- (Z + 2N) \bar{D}_d^L|^2 + |Z(A_1^R - A_2^L) - (2Z + N) \bar{D}_u^R| \\
&- (Z + 2N) \bar{D}_d^R|^2], \tag{58}
\end{aligned}$$

where

$$\bar{D}_q^L = D_q^L + \frac{Z_L^q + Z_R^q}{2} \frac{F_L}{m_Z^2 \sin^2 \theta_W \cos^2 \theta_W}, \tag{59}$$

$$\bar{D}_q^R = D_q^L|_{L \leftrightarrow R} \quad (q = u, d), \tag{60}$$

and Z and N denote the proton and neutron numbers in a nucleus, respectively. Z_{eff} has been determined in [6] and $F(q^2)$ is the nuclear form factor. In ${}^{48}_{22}\text{Ti}$, $Z_{\text{eff}} = 17.6$, $F(q^2 \simeq -m_\mu^2) \simeq 0.54$ [7].

IV. RESULTS OF THE NUMERICAL CALCULATIONS

In this section, we present results of our numerical analysis.

As was discussed in Sec. II, we assume universal scalar masses. Also for simplicity, we consider the so-called GUT relation among the gaugino masses:

$$\frac{M_1}{g_1^2} = \frac{M_2}{g_2^2} = \frac{M_3}{g_3^2}. \tag{61}$$

Then the SUSY-breaking terms have four free parameters: the universal scalar mass (m_0), the $SU(2)_L$ gaugino mass at low energies (M_2), the universal A parameter ($A = am_0$), and mixing parameter of the two Higgs bosons (B).

Concerning the SUSY invariant Higgs boson mass μ and B parameter which parametrize the mixing among h_1 and h_2 , we determined them so that the two Higgs doublets have correct vacuum expectation values $\langle h_1 \rangle = v \cos\beta/\sqrt{2}$ and

$\langle h_2 \rangle = v \sin \beta / \sqrt{2}$. With this radiative electroweak symmetry-breaking condition [4], we determine the mass spectra and mixing matrices of the superparticles. Then, we carefully investigate the parameter space where $\tan \beta$ is large and the masses of superparticles (especially sleptons and electroweak gauginos) are quite light enough to enhance the LFV rates. As a result, we found that there indeed exists a parameter space where the above conditions are satisfied. We checked, for $M_2 = 80$ GeV, that $\tan \beta$ can be as large as about 50.⁵ This result implies that there are regions in the parameter space where LFV processes have large branching ratios due to the large $\tan \beta$ enhancement mechanism.⁶

We also put constraints from experiments. Besides our requirement that the lightest superparticle be neutral, we use the consequences of negative searches for superparticles [8]. We also impose a constraint on the SUSY contribution to the anomalous magnetic dipole moment of the muon [11,12]. The experimental value of $\frac{1}{2}(g-2)$ is $1165923(8.4) \times 10^{-9}$ [8]. On the other hand, the theoretical prediction of the standard model is $11659180(15.3) \times 10^{-10}$ or $11659183(7.6) \times 10^{-10}$ [12], where the difference is due to different estimates of hadronic contributions. In our paper, we adopt the first one in order to derive a conservative bound. Therefore, the SUSY contribution should be constrained as

$$-26.7 \times 10^{-9} < (g-2)_\mu^{\text{SUSY}} < 46.7 \times 10^{-9}, \quad (62)$$

where a 2σ experimental error is considered. The SUSY contribution is shown in Fig. 7. Here, we take the parameter $a=0$ at the gravitational scale and $M_2=100$ GeV at low energies. The horizontal line is taken to be the left-handed selectron mass with a D -term contribution, which we denote by $m_{\tilde{e}_L}$. One finds that a significant region of the parameter space is excluded by this constraint in the large $\tan \beta$ region. This is because the same enhancement mechanism as the LFV processes works in the diagrams contributing to the $g-2$. For completeness, we will give formulas of the contribution of the superparticle loops to the anomalous magnetic dipole moment in Appendix C.

Let us now discuss the branching ratios for each LFV process. First we consider the case where the neutrino mixing matrix is described by the KM matrix.

A. Case (1): $V = V_{\text{KM}}$

As in the first trial, we shall consider the case where $V = V_{\text{KM}}$, where we take $s_{12} = 0.22$, $s_{23} = 0.04$, and

$$m_L^2 \simeq \begin{pmatrix} 1.00 & (0.30-0.43) \times 10^{-4} & -(0.74-1.07) \times 10^{-3} \\ (0.30-0.43) \times 10^{-4} & 1.00 & -(0.54-0.78) \times 10^{-2} \\ -(0.74-1.07) \times 10^{-3} & -(0.54-0.78) \times 10^{-2} & 0.77-0.80 \end{pmatrix} \times m_0^2, \quad (63)$$

⁵Throughout this paper, we take the top quark mass $m_t = 174$ GeV [8]. Also we take the bottom quark mass $m_b = 4.25$ GeV [9], which corresponds to 3.1 GeV at the Z mass scale.

⁶Note that the situation here contrasts to the case of Yukawa unification where the radiative breaking with the universal scalar mass requires a heavy superparticle spectrum, larger than, say, 500 GeV [10].

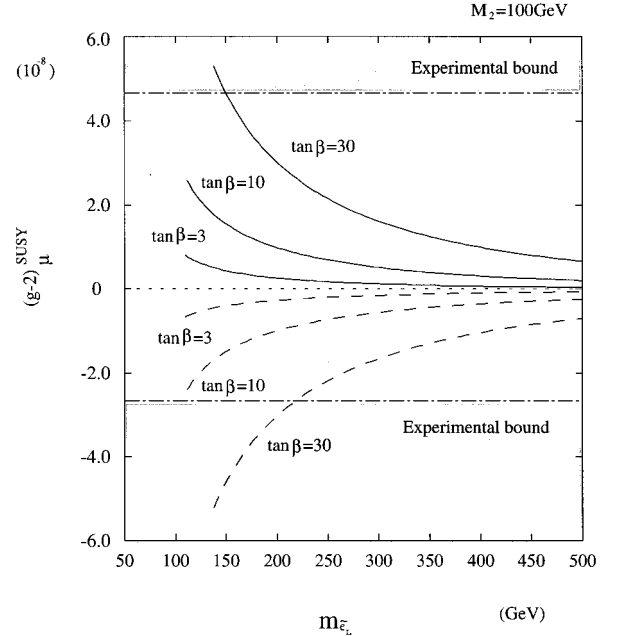


FIG. 7. The values of the SUSY contribution to the anomalous magnetic dipole moment of muons $(g-2)_\mu^{\text{SUSY}}$ as a function of the left-handed selectron mass with the D -term contribution, which we denote by $m_{\tilde{e}_L}$. Here we assume $a=0$ at the gravitational scale. Real lines correspond to the case for $\mu > 0$, while dashed lines for $\mu < 0$. Here we have taken $M_2 = 100$ GeV and $\tan \beta = 3, 10, 30$. The shaded regions are excluded by the present experiments.

$s_{13} = 0.0035$ in the standard notation [8]. We ignore the possible Kobayashi-Maskawa complex phase and consider V to be real, for simplicity. The eigenvalues of the neutrino Yukawa couplings are assumed to be equal to those of up-type quarks at the gravitational scale. Since the magnitude of the top quark Yukawa coupling is close to its perturbative bound, this ansatz will maximize the magnitude of LFV in the slepton mass matrix. Also, to determine the right-handed neutrino Majorana mass M_R , we fix the τ neutrino mass at 10 eV so that it constitutes the hot component of the dark matter of the Universe. In this case, M_R is about 10^{12-13} GeV.

Solving the RGE's numerically, we obtain the mass squared matrix for the $SU(2)_L$ doublet sleptons at the electroweak scale:

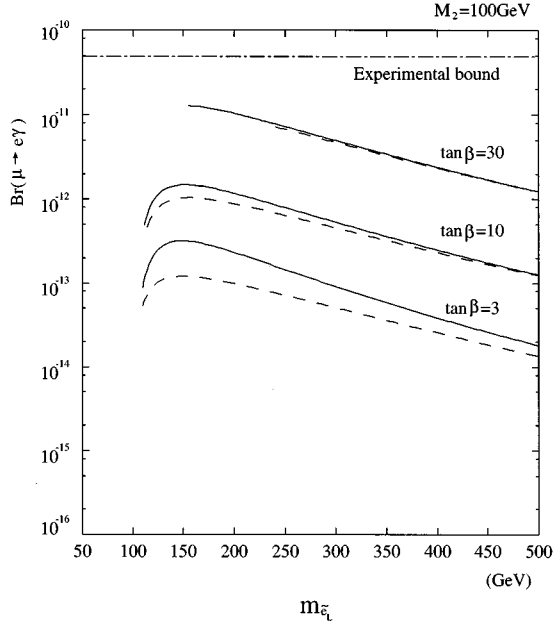


FIG. 8. Branching ratios for the process $\mu \rightarrow e\gamma$ in the case (1) $V = V_{\text{KM}}$ as a function of the left-handed selectron mass with the D -term contribution, $m_{\tilde{e}_L}$. Real lines correspond to the case for $\mu > 0$, while dashed lines for $\mu < 0$. Here we have taken $M_2 = 100$ GeV and $\tan\beta = 3, 10, 30$. We also show the present experimental upper bound for this process by the dash-dotted line.

where $\tan\beta$ varies from 3 to 30, $M_2 = 0$, and $a = 0$. For a nonvanishing M_2 , the diagonal elements of the above matrix become larger and the flavor-violating off-diagonal elements become relatively less important, as the gaugino mass gets larger. The effect of a nonvanishing a parameter can be seen from Eq. (7), which does not change the result drastically. In the following numerical calculations we will take $a = 0$.

We find that in Eq. (63) the off-diagonal elements in the mass matrix are small. This is because the off-diagonal slepton masses are proportional to $V_{3i}^* V^{3j}$ in the case of hierarchical neutrino masses, which are small if we assume that V is equal to the KM matrix. Nevertheless, as will be shown shortly, the enhancement in the large $\tan\beta$ region yields large branching ratios for the LFV processes, which are close to the present experimental upper bounds.

1. $\mu \rightarrow e\gamma$

The result of our computation on the branching ratio $B(\mu \rightarrow e\gamma)$ is shown in Fig. 8 for $M_2 = 100$ GeV. The horizontal line is taken to be the left-handed selectron mass with the D -term contribution, $m_{\tilde{e}_L}$. Real lines are for $\mu > 0$, while dashed lines are for $\mu < 0$. We find that the branching ratios are rather insensitive to the choice of the sign of the μ parameter, in particular when $\tan\beta$ is large. For the large $\tan\beta$ case, some regions of small slepton masses are excluded by the constraint from $g - 2$. As can be seen from Fig. 7, it is less stringent for the $\mu > 0$ case than the $\mu < 0$ case.⁷

⁷Here, we should comment that the SUSY contribution to the $b \rightarrow s\gamma$ process is also significant and some part of the parameter

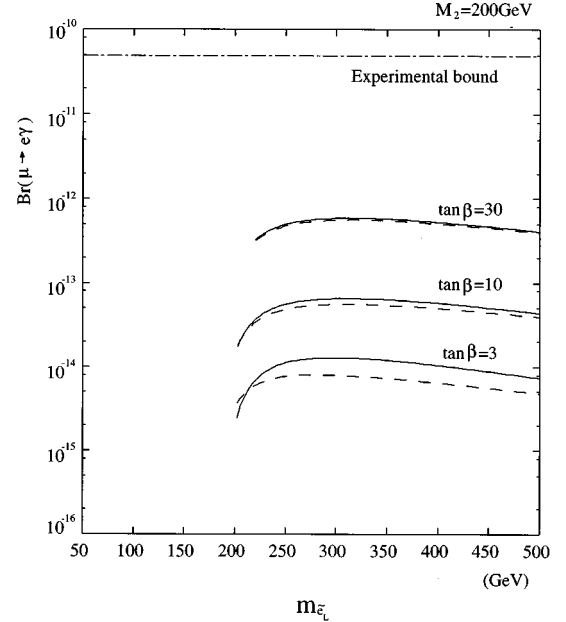


FIG. 9. Same as Fig. 8 except for $M_2 = 200$ GeV.

One can see that even if we impose this constraint, the branching ratio can be as large as 10^{-11} , which is very close to the present experimental bound $B(\mu \rightarrow e\gamma)|_{\text{expt}} < 4.9 \times 10^{-11}$. For smaller values of $\tan\beta$, the branching ratio reduces, obeying $\propto \tan^2\beta$.

We compared the chargino loop contribution with the neutralino loop contribution and found that the former dominates. This is important when we compare our results with the case of SU(5) grand unification. (See Sec. V.)

In Fig. 9, we show the case of $M_2 = 200$ GeV. The maximum of the branching ratio is about 10^{-12} for $\tan\beta = 30$, about one order of magnitude smaller than the $M_2 = 100$ GeV case. We also studied the case $M_2 = 80$ GeV, and found that the branching ratio is about a factor of 2 larger than the $M_2 = 100$ GeV case.

2. $\mu^- \rightarrow e^- e^- e^+$

Next, let us consider the process $\mu^- \rightarrow e^- e^- e^+$. Currently the experimental upper bound on the branching ratio of this process is 1.0×10^{-12} [8]. We show the results of our calculation to this process in Fig. 10 for $M_2 = 100$ GeV. The branching ratio has the maximum of $\sim 10^{-13}$ for large $\tan\beta$ with small gaugino mass. One can check that this process is dominated by penguin-type diagrams. Indeed compared with the branching ratio of $\mu \rightarrow e\gamma$, one finds a simple relation

space should be excluded [12–14]. However, it is complicated to estimate the SUSY contribution to the $b \rightarrow s\gamma$ process, since the chargino loop can contribute either constructively or destructively to the others, especially the charged Higgs boson loop. Thus, it seems to us that to determine which regions of the parameter space are really eliminated contains some delicate issues as discussed by Ref. [14]. We believe that such an analysis is out of the scope of our paper. Thus, we do not use the constraint from the $b \rightarrow s\gamma$ process.

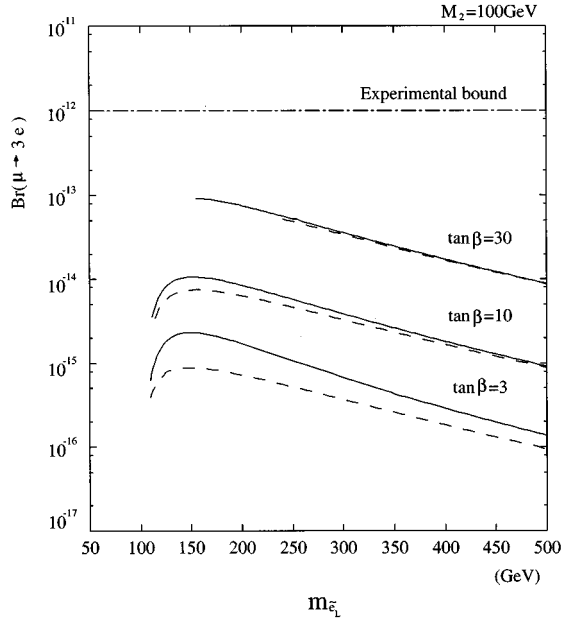


FIG. 10. Branching ratios for the process $\mu^- \rightarrow e^- e^- e^+$ in the case (1) $V=V_{\text{KM}}$ as a function of the left-handed selectron mass with the D -term contribution, $m_{\tilde{e}_L}$. Real lines correspond to the case for $\mu > 0$, while dashed lines for $\mu < 0$. Here we have taken $M_2 = 100$ GeV and $\tan\beta = 3, 10, 30$. We also show the present experimental upper bound for this process by the dash-dotted line.

$$\frac{B(\mu \rightarrow 3e)}{B(\mu \rightarrow e\gamma)} \sim 7 \times 10^{-3}, \quad (64)$$

which is in agreement with the ratio expected by the dominance of the penguin-type diagrams, Eq. (57).

3. μ - e conversion in ${}^{48}\text{Ti}$

Experimentally, the μ - e conversion rate in nuclei is also constrained strongly. The experimental upper bound on the conversion rate with the target ${}^{48}\text{Ti}$ reaches 4.3×10^{-12} [8]. We show the results of our calculation to this process in Fig. 11 for $M_2 = 100$ GeV. The branching ratio takes its maximal value of $\sim 10^{-13}$ in the parameter region where $\tan\beta$ is large and the gaugino masses are small. On the other hand, for small $\tan\beta$ and $\mu < 0$ a cancellation among the diagrams occurs and the event rate damps rapidly. The penguin-type diagram is not dominant in the small $\tan\beta$ region because there is not the same logarithmic enhancement as $\mu^- \rightarrow e^- e^- e^+$.

4. $\tau \rightarrow \mu \gamma$

Finally we present our result for $\tau \rightarrow \mu \gamma$ in Fig. 12. We find that, with $M_2 = 100$ GeV, the branching ratio is as large as 10^{-7} , one and a half orders of magnitude smaller than the present experimental bound $B(\tau \rightarrow \mu \gamma)|_{\text{expt}} < 4.2 \times 10^{-6}$ [8]. Similar to the case of $\mu \rightarrow e \gamma$, it can be seen that the branching ratio is proportional to $\tan\beta$ squared.

B. Case (2): Neutrino mixing implied by the atmospheric neutrino deficit

A class of solutions to the atmospheric and solar neutrino deficits requires a maximal mixing of the τ and muon neu-

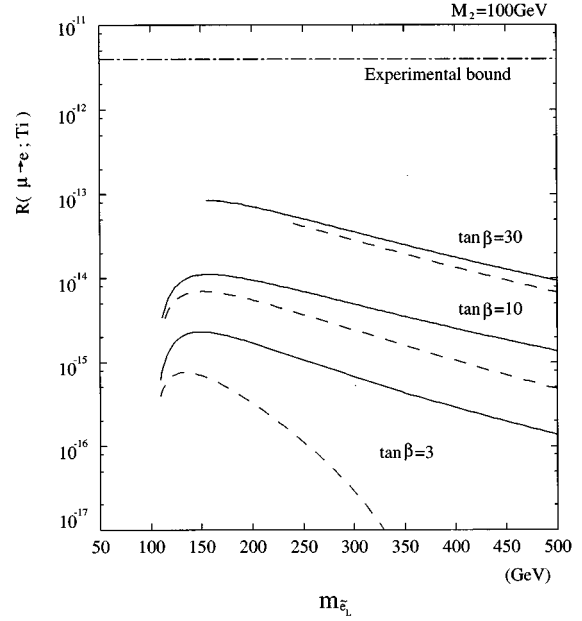


FIG. 11. The μ - e conversion rates in nuclei ${}^{48}\text{Ti}$ in the case (1) $V=V_{\text{KM}}$ as a function of the left-handed selectron mass with the D -term contribution, $m_{\tilde{e}_L}$. Real lines correspond to the case for $\mu > 0$, while dashed lines for $\mu < 0$. Here we have taken $M_2 = 100$ GeV and $\tan\beta = 3, 10, 30$. We also show the present experimental upper bound for this process by the dash-dotted line.

trinos, yielding a large off-diagonal element in the slepton mass matrix. The neutrino mixing matrix we take in this example is

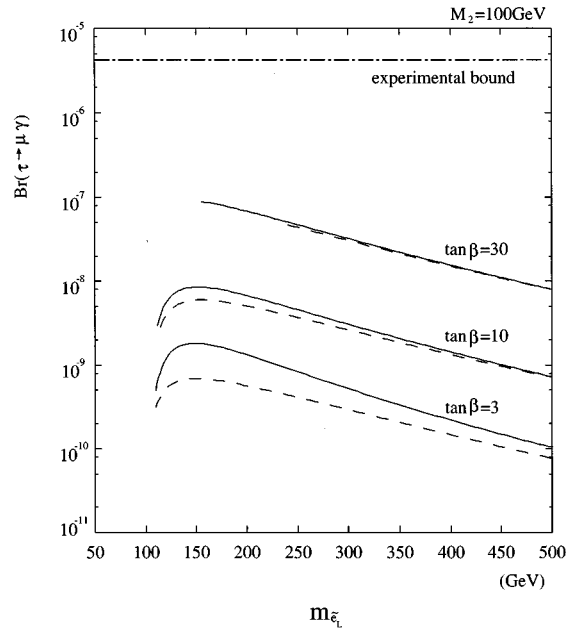


FIG. 12. Branching ratios for the process $\tau \rightarrow \mu \gamma$ in the case (1) $V=V_{\text{KM}}$ as a function of the left-handed selectron mass with the D -term contribution, $m_{\tilde{e}_L}$. Real lines correspond to the case for $\mu > 0$, while dashed lines for $\mu < 0$. Here we have taken $M_2 = 100$ GeV and $\tan\beta = 3, 10, 30$. We also show the present experimental upper bound for this process by the dash-dotted line.

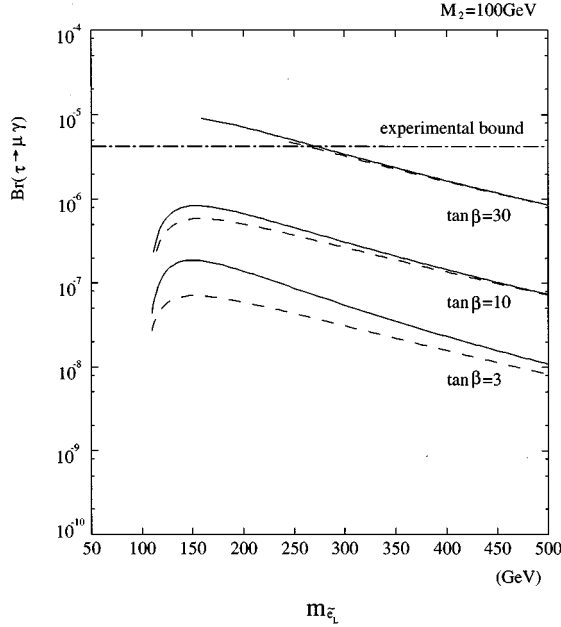


FIG. 13. Branching ratios for the process $\tau \rightarrow \mu \gamma$ in the case (2) neutrino mixing implied by atmospheric neutrino deficit, as a function of the left-handed selectron mass with the D -term contribution, $m_{\tilde{e}_L}$. Real lines correspond to the case for $\mu > 0$, while dashed lines for $\mu < 0$. Here we have taken $M_2 = 100$ GeV and $\tan\beta = 3, 10, 30$. We also show the present experimental upper bound for this process by the dash-dotted line.

$$V \simeq \begin{pmatrix} 1.00 & 0.87 \times 10^{-1} & - \\ -0.66 \times 10^{-1} & 0.755 & 0.656 \\ - & -0.656 & 0.755 \end{pmatrix}, \quad (65)$$

and the τ neutrino mass is assumed to be 0.4 eV [15]. Here, we only consider the generation mixing of the second and third generations and ignore the others. The (1,3) and (3,1) elements of the mixing matrix cannot be determined from the solar and atmospheric neutrino deficits. This uncertainty, however, does not matter if we only consider the LFV process among the second and third generations. As in case (1), we assume that the magnitude of the third-generation neutrino Yukawa coupling $f_{\nu 3}$ is equal to the top quark Yukawa coupling at the gravitational scale. The latter choice will give us a maximum violation of LFV in the slepton mass matrix.

The result for $B(\tau \rightarrow \mu \gamma)$ is shown in Fig. 13. We find that in some portion of the parameter space, the branching ratio exceeds the present experimental upper bound, in particular when $\tan\beta$ is large and the superparticles are light.

V. CONCLUSIONS AND DISCUSSION

In this paper, we have considered LFV in the minimal supersymmetric standard model (MSSM) with right-handed neutrino multiplets. In the presence of the Yukawa couplings of the right-handed neutrinos, the left-handed slepton mass matrix m_L^2 loses its universal property even if we assume the minimal-supergravity-type boundary condition on sfermion masses. In our case, because of the renormalization effect, as

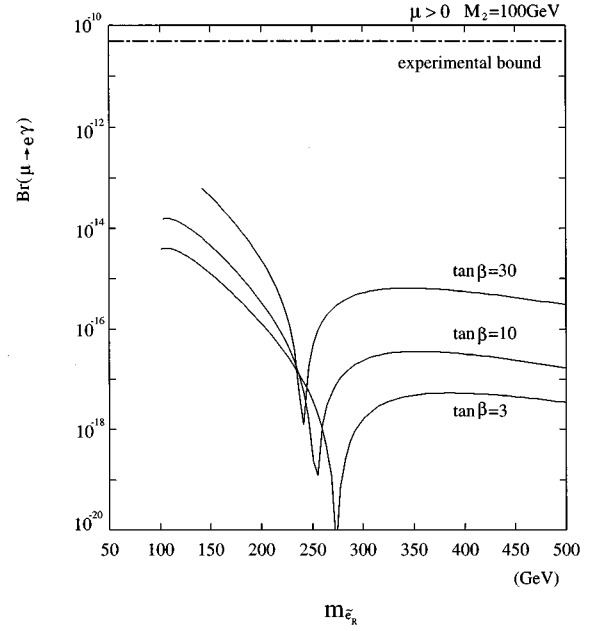


FIG. 14. Branching ratios for the process $\mu \rightarrow e \gamma$ in the case for the minimal SU(5) grand unified theory, as a function of the right-handed selectron mass with the D -term contribution, $m_{\tilde{e}_R}$. Here we have taken $\mu > 0$, $M_2 = 100$ GeV, and $\tan\beta = 3, 10, 30$. We also show the present experimental upper bound for this process by the dash-dotted line.

can be seen from Eq. (63), we obtain LFV in m_L^2 as well as a smaller value of the (3,3) element of m_L^2 compared with the other diagonal elements, which is a typical feature of the case with right-handed neutrinos [16]. We have calculated the interaction rates for the various LFV processes with the full diagonalization of the slepton mass matrices and of the chargino and neutralino mass matrices. We emphasized the enhancement of the interaction rates for large $\tan\beta$, the ratio of the vacuum expectation values (VEV's) of the two Higgs doublets. This enhancement originates from the fact that there is freedom to pick up one of two vacuum expectation values in the MSSM in the magnetic-dipole-moment-type diagrams. For example, for the process $l_j \rightarrow l_i \gamma$, diagrams of the type Fig. 1(c) and Fig. 2 give the enhancement. Even when the mixing matrix in the lepton sector has a similar structure as the KM matrix of the quark sector, the enhancement mechanism can make the branching ratios close to the present experimental bounds.

It is interesting to compare the LFV processes induced by the right-handed neutrino Yukawa couplings with those in the minimal SU(5) grand unified theory [17,18]. In the latter case, the renormalization-group flow above the GUT scale results in LFV in the SU(2)_L singlet (right-handed) slepton masses. Let us consider, for example, the resulting branching ratio of $\mu \rightarrow e \gamma$. The diagrams which will give the enhancement in the large $\tan\beta$ region are similar to Figs. 1(c) and 2(a). The important difference from the previous case is in Fig. 2. Now, only diagrams involving the B -ino contribute, since the W -ino does not couple to the singlet sleptons. In this case, we can see that contributions coming from the two diagrams Fig. 1(c) and Fig. 2(a) have opposite signs, and

thus partially cancel out with each other. The numerical result is shown in Fig. 14. The horizontal line is the mass of the right-handed selectron with the D -term contribution, $m_{\tilde{e}_R}$. Here, we have taken $M_2 = 100$ GeV. The branching ratio never exceeds 10^{-13} , more than two orders of magnitude beneath the present experimental upper bound. Also one finds regions where the branching ratio becomes very small due to the cancellation explained above.

What happens if the standard model with right-handed neutrinos is embedded in the framework of SU(5) GUT? In this case, both the mass matrix of the left-handed sleptons and that of the right-handed ones have LFV. The situation is quite similar to the case of SO(10) GUT [18,19]. For example, if we consider the $\mu \rightarrow e \gamma$, the dominant diagram will be similar to Fig. 1(c), which, however, picks up $(m_{LR}^2)_3^3$, proportional to the τ -lepton mass. Thus we expect further enhancement in the branching ratio by $(m_\tau/m_\mu)^2$ compared to the case we studied in this paper.

To conclude our paper, we should emphasize that the branching ratios of LFV processes induced by right-handed neutrino Yukawa couplings can be close to the present ex-

perimental bounds and can be within the reach of future experiments. Efforts to search for these LFV signals should be encouraged.

ACKNOWLEDGMENTS

We would like to thank T. Yanagida for useful discussions. We are also grateful to T. Goto and P. Nath for discussion on the $b \rightarrow s \gamma$ process, and to S. Orito for a comment on the anomalous magnetic dipole moment of the muon. One of authors (J.H.) thanks the Japan Society for the Promotion of Science for financial support.

APPENDIX A: RENORMALIZATION GROUP EQUATIONS

In this appendix, we give the one-loop renormalization-group equations (RGE's) for the Yukawa couplings and the soft SUSY-breaking terms in the scalar potential. The RGE's for the gauge coupling constants and the gaugino masses are unchanged at the one-loop level, since the right-handed neutrinos are singlet under standard-model gauge symmetry. Yukawa coupling constants:

$$\mu \frac{d}{d\mu} f_l^{ij} = \frac{1}{16\pi^2} \left[\left\{ -\frac{9}{5} g_1^2 - 3g_2^2 + 3\text{Tr}(f_d f_d^\dagger) + \text{Tr}(f_l f_l^\dagger) \right\} f_l^{ij} + 3(f_l f_l^\dagger f_l)^{ij} + (f_l f_w^\dagger f_\nu)^{ij} \right], \quad (\text{A1})$$

$$\mu \frac{d}{d\mu} f_\nu^{ij} = \frac{1}{16\pi^2} \left[\left\{ -\frac{3}{5} g_1^2 - 3g_2^2 + 3\text{Tr}(f_w f_w^\dagger) + \text{Tr}(f_\nu f_\nu^\dagger) \right\} f_\nu^{ij} + 3(f_w f_w^\dagger f_\nu)^{ij} + (f_w f_l^\dagger f_l)^{ij} \right]. \quad (\text{A2})$$

Soft breaking terms:

$$\mu \frac{d}{d\mu} (m_{\tilde{L}}^2)_i^j = \frac{1}{16\pi^2} \left[(m_{\tilde{L}}^2 f_l^\dagger f_l + f_l^\dagger f_l m_{\tilde{L}}^2)_i^j + (m_{\tilde{L}}^2 f_\nu^\dagger f_\nu + f_\nu^\dagger f_\nu m_{\tilde{L}}^2)_i^j + 2(f_l^\dagger m_{\tilde{e}}^2 f_l + \tilde{m}_{h1}^2 f_l^\dagger f_l + A_l^\dagger A_l)_i^j + 2(f_\nu^\dagger m_{\tilde{\nu}}^2 f_\nu + \tilde{m}_{h2}^2 f_\nu^\dagger f_\nu + A_\nu^\dagger A_\nu)_i^j - \left(\frac{6}{5} g_1^2 |M_1|^2 + 6g_2^2 |M_2|^2 \right) \delta_i^j - \frac{3}{5} g_1^2 S \delta_i^j \right], \quad (\text{A3})$$

$$\mu \frac{d}{d\mu} (m_{\tilde{e}}^2)_j^i = \frac{1}{16\pi^2} \left[2(m_{\tilde{e}}^2 f_l^\dagger f_l + f_l f_l^\dagger m_{\tilde{e}}^2)_j^i + 4(f_l m_{\tilde{L}}^2 f_l^\dagger + \tilde{m}_{h1}^2 f_l f_l^\dagger + A_l A_l^\dagger)_j^i - \frac{24}{5} g_1^2 |M_1|^2 \delta_j^i + \frac{6}{5} g_1^2 S \delta_j^i \right],$$

$$\mu \frac{d}{d\mu} (m_{\tilde{\nu}}^2)_j^i = \frac{1}{16\pi^2} [2(m_{\tilde{\nu}}^2 f_w^\dagger f_w + f_w f_w^\dagger m_{\tilde{\nu}}^2)_j^i + 4(f_w m_{\tilde{L}}^2 f_w^\dagger + \tilde{m}_{h2}^2 f_w f_w^\dagger + A_\nu A_\nu^\dagger)_j^i], \quad (\text{A4})$$

$$\mu \frac{d}{d\mu} A_l^{ij} = \frac{1}{16\pi^2} \left[\left\{ -\frac{9}{5} g_1^2 - 3g_2^2 + 3\text{Tr}(f_d^\dagger f_d) + \text{Tr}(f_l^\dagger f_l) \right\} A_l^{ij} + 2 \left\{ -\frac{9}{5} g_1^2 M_1 - 3g_2^2 M_2 + 3\text{Tr}(f_d^\dagger A_d) + \text{Tr}(f_l^\dagger A_l) \right\} f_l^{ij} + 4(f_l f_l^\dagger A_l)^{ij} + 5(A_l f_l^\dagger f_l)^{ij} + 2(f_l f_\nu^\dagger A_\nu)^{ij} + (A_l f_w^\dagger f_\nu)^{ij} \right], \quad (\text{A5})$$

$$\mu \frac{d}{d\mu} A_\nu^{ij} = \frac{1}{16\pi^2} \left[\left\{ -\frac{3}{5} g_1^2 - 3g_2^2 + 3\text{Tr}(f_w^\dagger f_w) + \text{Tr}(f_\nu^\dagger f_\nu) \right\} A_\nu^{ij} + 2 \left\{ -\frac{3}{5} g_1^2 M_1 - 3g_2^2 M_2 + 3\text{Tr}(f_w^\dagger A_w) + \text{Tr}(f_\nu^\dagger A_\nu) \right\} f_\nu^{ij} + 4(f_w f_\nu^\dagger A_\nu)^{ij} + 5(A_w f_w^\dagger f_\nu)^{ij} + 2(f_w f_l^\dagger A_l)^{ij} + (A_w f_l^\dagger f_l)^{ij} \right], \quad (\text{A6})$$

where

$$S = \text{Tr}(m_Q^2 + m_d^2 - 2m_u^2 - m_L^2 + m_e^2) - \tilde{m}_{h1}^2 + \tilde{m}_{h2}^2. \quad (\text{A7})$$

Here, we followed the GUT convention for the normalization of the $U(1)_Y$ gauge coupling constant g_1 , such as $g_Y^2 = \frac{3}{5} g_1^2$.

APPENDIX B: INTERACTION OF GAUGINOS, SFERMIONS, AND FERMIONS

In this appendix, we give our notations and conventions adopted in Sec. III and give vertices relevant for our calculation.

Let us first discuss fermions. We denote by l_i , u_i , and d_i the fermion mass eigenstates with the obvious meaning. The subscript i ($i=1,2,3$) represents the generation. As for the neutrinos, their masses are small and negligible. In our convention, ν_i is the $SU(2)_L$ isodoublet partner to e_{Li} .

Next we consider sfermions. Let \tilde{f}_{Li} and \tilde{f}_{Ri} be the superpartners of f_{Li} and f_{Ri} , respectively. Here, f stands for l , u , or d . The mass matrix for the sfermions can be written in the form

$$(\tilde{f}_L^\dagger, \tilde{f}_R^\dagger) \begin{pmatrix} m_L^2 & m_{LR}^{2T} \\ m_{LR}^2 & m_R^2 \end{pmatrix} \begin{pmatrix} \tilde{f}_L \\ \tilde{f}_R \end{pmatrix}, \quad (\text{B1})$$

where m_L^2 and m_R^2 are 3×3 Hermitian matrices and m_{LR}^2 is a 3×3 matrix. These elements are given from Eqs. (1), (3) as

$$m_L^2 = m_{\tilde{f}_L}^2 + m_f^2 + m_Z^2 \cos 2\beta (T_{3L}^f - Q_{\text{em}}^f \sin^2 \theta_W), \quad (\text{B2})$$

$$m_R^2 = m_{\tilde{f}_R}^2 + m_f^2 - m_Z^2 \cos 2\beta (T_{3R}^f - Q_{\text{em}}^f \sin^2 \theta_W), \quad (\text{B3})$$

$$m_{LR}^2 = \begin{cases} -A_f \nu \sin \beta / \sqrt{2} - m_f \mu \cot \beta & (f=u), \\ A_f \nu \cos \beta / \sqrt{2} - m_f \mu \tan \beta & (f=d, l), \end{cases} \quad (\text{B4})$$

where $T_{3L(R)}^f$ and Q_{em}^f are weak isospin and electric charge, respectively. Here, $m_{\tilde{f}_L}^2 = m_Q^2$ for squarks, $m_{\tilde{f}_L}^2 = m_L^2$ for sleptons, and $m_{\tilde{f}_R}^2$ are each right-handed sfermion soft breaking masses. We assume the above mass matrix to be real. This is, in general, not diagonal and includes mixing between different generations. We diagonalize the mass matrix \mathcal{M}^2 by a 6×6 real orthogonal matrix U^f as

$$U^f \mathcal{M}^2 U^{fT} = (\text{diagonal}), \quad (\text{B5})$$

and we denote its eigenvalues by $m_{\tilde{f}_X}^2$ ($X=1, \dots, 6$). The mass eigenstate is then written as

$$\tilde{f}_X = U_{X,i}^f \tilde{f}_{Li} + U_{X,i+3}^f \tilde{f}_{Ri} \quad (X=1, \dots, 6). \quad (\text{B6})$$

Conversely, we have

$$\tilde{f}_{Li} = U_{iX}^{fT} \tilde{f}_X = U_{Xi}^f \tilde{f}_X, \quad (\text{B7})$$

$$\tilde{f}_{Ri} = U_{i+3,X}^{fT} \tilde{f}_X = U_{X,i+3}^f \tilde{f}_X. \quad (\text{B8})$$

Attention should be paid to the neutrinos since there is no right-handed sneutrino in the MSSM. Let $\tilde{\nu}_{Li}$ be the superpartner of the neutrino ν_i . The mass eigenstate $\tilde{\nu}_X$ ($X=1,2,3$) is related to $\tilde{\nu}_{Li}$ as

$$\tilde{\nu}_{Li} = U_{Xi}^\nu \tilde{\nu}_X. \quad (\text{B9})$$

We now turn to charginos. The mass matrix of the charginos is given by

$$-\mathcal{L}_m = (\overline{\tilde{W}_R^-} \quad \overline{\tilde{H}_{2R}^-}) \begin{pmatrix} M_2 & \sqrt{2} m_W \cos \beta \\ \sqrt{2} m_W \sin \beta & \mu \end{pmatrix} \begin{pmatrix} \tilde{W}_L^- \\ \tilde{H}_{1L}^- \end{pmatrix} + \text{H.c.} \quad (\text{B10})$$

This matrix M_C is diagonalized by 2×2 real orthogonal matrices O_L and O_R as

$$O_R M_C O_L^T = (\text{diagonal}). \quad (\text{B11})$$

Define

$$\begin{pmatrix} \tilde{\chi}_{1L}^- \\ \tilde{\chi}_{2L}^- \end{pmatrix} = O_L \begin{pmatrix} \tilde{W}_L^- \\ \tilde{H}_{1L}^- \end{pmatrix}, \quad \begin{pmatrix} \tilde{\chi}_{1R}^- \\ \tilde{\chi}_{2R}^- \end{pmatrix} = O_R \begin{pmatrix} \tilde{W}_R^- \\ \tilde{H}_{2R}^- \end{pmatrix}. \quad (\text{B12})$$

Then

$$\tilde{\chi}_A^- = \tilde{\chi}_{AL}^- + \tilde{\chi}_{AR}^- \quad (A=1,2), \quad (\text{B13})$$

forms a Dirac fermion with mass $M_{\tilde{\chi}_A^-}$.

Finally we consider neutralinos. The mass matrix of the neutralino sector is given by

$$-\mathcal{L}_m = \frac{1}{2} (\tilde{B}_L \tilde{W}_L^0 \tilde{H}_{1L}^0 \tilde{H}_{2L}^0) M_N \begin{pmatrix} \tilde{B}_L \\ \tilde{W}_L^0 \\ \tilde{H}_{1L}^0 \\ \tilde{H}_{2L}^0 \end{pmatrix} + \text{H.c.}, \quad (\text{B14})$$

where

$$M_N = \begin{pmatrix} M_1 & 0 & -m_Z \sin \theta_W \cos \beta & m_Z \sin \theta_W \sin \beta \\ 0 & M_2 & m_Z \cos \theta_W \cos \beta & -m_Z \cos \theta_W \sin \beta \\ -m_Z \sin \theta_W \cos \beta & m_Z \cos \theta_W \cos \beta & 0 & -\mu \\ m_Z \sin \theta_W \sin \beta & -m_Z \cos \theta_W \sin \beta & -\mu & 0 \end{pmatrix}. \quad (\text{B15})$$

The diagonalization is done by a real orthogonal matrix O_N :

$$O_N M_N O_N^T = \text{diagonal}. \quad (\text{B16})$$

The mass eigenstates are given by

$$\tilde{\chi}_{AL}^0 = (O_N)_{AB} \tilde{X}_{BL}^0 \quad (A, B = 1, \dots, 4), \quad (\text{B17})$$

where

$$\tilde{X}_{AL}^0 = (\tilde{B}_L, \tilde{W}_L, \tilde{H}_{1L}^0, \tilde{H}_{2L}^0). \quad (\text{B18})$$

We have thus Majorana spinors

$$\tilde{\chi}_A^0 = \tilde{\chi}_{AL}^0 + \tilde{\chi}_{AR}^0 \quad (A = 1, \dots, 4), \quad (\text{B19})$$

with mass $M_{\tilde{\chi}_A^0}$.

We now give the interaction Lagrangian of fermions, sfermions, and charginos,

$$\begin{aligned} \mathcal{L}_{\text{int}} = & \bar{l}_i (C_{iAX}^{R(l)} P_R + C_{iAX}^{L(l)} P_L) \tilde{\chi}_A^- \tilde{\nu}_X + \bar{\nu}_i (C_{iAX}^{R(\nu)} P_R \\ & + C_{iAX}^{L(\nu)} P_L) \tilde{\chi}_A^+ \tilde{l}_X + \bar{d}_i (C_{iAX}^{R(d)} P_R + C_{iAX}^{L(d)} P_L) \tilde{\chi}_A^- \tilde{u}_X \\ & + \bar{u}_i (C_{iAX}^{R(u)} P_R + C_{iAX}^{L(u)} P_L) \tilde{\chi}_A^+ \tilde{d}_X + \text{H.c.}, \end{aligned} \quad (\text{B20})$$

where the coefficients are

$$C_{iAX}^{R(l)} = -g_2 (O_R)_{A1} U_{X,i}^{\nu},$$

$$C_{iAX}^{L(l)} = g_2 \frac{m_{l_i}}{\sqrt{2} m_W \cos \beta} (O_L)_{A2} U_{X,i}^{\nu}, \quad C_{iAX}^{R(\nu)} = -g_2 (O_L)_{A1} U_{X,i}^l,$$

$$C_{iAX}^{L(\nu)} = g_2 \frac{m_{l_i}}{\sqrt{2} m_W \cos \beta} (O_L)_{A2} U_{X,i+3}^l,$$

$$C_{iAX}^{R(d)} = g_2 \left\{ -(O_R)_{A1} U_{X,i}^u + \frac{m_{u_i}}{\sqrt{2} m_W \sin \beta} (O_R)_{A2} U_{X,i+3}^u \right\},$$

$$C_{iAX}^{L(d)} = g_2 \frac{m_{d_i}}{\sqrt{2} m_W \cos \beta} (O_L)_{A2} U_{X,i}^u,$$

$$C_{iAX}^{R(u)} = g_2 \left\{ -(O_L)_{A1} U_{X,i}^d + \frac{m_{d_i}}{\sqrt{2} m_W \cos \beta} (O_L)_{A2} U_{X,i+3}^d \right\},$$

$$C_{iAX}^{L(u)} = g_2 \frac{m_{u_i}}{\sqrt{2} m_W \sin \beta} (O_R)_{A2} U_{X,i}^d. \quad (\text{B21})$$

The interaction Lagrangian of fermions, sfermions, and neutralinos is similarly written as

$$\mathcal{L}_{\text{int}} = \bar{f}_i (N_{iAX}^{R(f)} P_R + N_{iAX}^{L(f)} P_L) \tilde{\chi}_A^0 \tilde{f}_X, \quad (\text{B22})$$

where f stands for l , ν , d , and u . The coefficients are

$$N_{iAX}^{R(l)} = -\frac{g_2}{\sqrt{2}} \left\{ [-(O_N)_{A2} - (O_N)_{A1} \tan \theta_W] U_{X,i}^l + \frac{m_{l_i}}{m_W \cos \beta} (O_N)_{A3} U_{X,i+3}^l \right\},$$

$$N_{iAX}^{L(l)} = -\frac{g_2}{\sqrt{2}} \left\{ \frac{m_{l_i}}{m_W \cos \beta} (O_N)_{A3} U_{X,i}^l + 2(O_N)_{A1} \tan \theta_W U_{X,i+3}^l \right\}, \quad N_{iAX}^{R(\nu)} = -\frac{g_2}{\sqrt{2}} [(O_N)_{A2} - (O_N)_{A1} \tan \theta_W] U_{X,i}^{\nu},$$

$$N_{iAX}^{L(\nu)} = 0,$$

$$N_{iAX}^{R(d)} = -\frac{g_2}{\sqrt{2}} \left\{ [-(O_N)_{A2} + \frac{1}{3} (O_N)_{A1} \tan \theta_W] U_{X,i}^d + \frac{m_{d_i}}{m_W \cos \beta} (O_N)_{A3} U_{X,i+3}^d \right\},$$

$$N_{iAX}^{L(d)} = -\frac{g_2}{\sqrt{2}} \left\{ \frac{m_{d_i}}{m_W \cos \beta} (O_N)_{A3} U_{X,i}^d + \frac{2}{3} \tan \theta_W (O_N)_{A1} U_{X,i+3}^d \right\},$$

$$N_{iAX}^{R(u)} = -\frac{g_2}{\sqrt{2}} \left\{ [(O_N)_{A2} + \frac{1}{3} (O_N)_{A1} \tan \theta_W] U_{X,i}^u + \frac{m_{u_i}}{m_W \sin \beta} (O_N)_{A4} U_{X,i+3}^u \right\},$$

$$N_{iAX}^{L(u)} = -\frac{g_2}{\sqrt{2}} \left\{ \frac{m_{u_i}}{m_W \sin\beta} (O_N)_{A4} U_{X,i}^u - \frac{4}{3} \tan\theta_W (O_N)_{A1} U_{X,i+3}^u \right\}. \quad (\text{B23})$$

APPENDIX C: ANOMALOUS MAGNETIC DIPOLE MOMENT OF THE MUON

The magnetic dipole moment interaction of the muon is written

$$\frac{ie}{2m_\mu} F(q^2) \bar{u}(p_f) \sigma_{\mu\nu} q^\mu \epsilon^\nu u(p_i), \quad (\text{C1})$$

where $q = p_f - p_i$ and ϵ the polarization vector of the external photon. Then, the anomalous magnetic dipole moment of muon is

$$(g-2)_\mu \equiv 2F(q^2=0). \quad (\text{C2})$$

We can write SUSY contributions as $(g-2)_\mu^{\text{SUSY}} = (g^{(C)} + g^{(N)})_\mu$. The first term $g_\mu^{(C)}$ represents the chargino-loop contribution as

$$g_\mu^{(C)} = \frac{1}{48\pi^2} \frac{m_\mu^2}{m_{\tilde{\nu}_X}^2} |C_{2AX}^{L(l)}|^2 \frac{2+3x_{AX}-6x_{AX}^2+x_{AX}^3+6x_{AX}\ln x_{AX}}{(1-x_{AX})^4} + \frac{1}{16\pi^2} \frac{m_\mu M_{\tilde{\chi}_A^-}}{m_{\tilde{\nu}_X}^2} C_{2AX}^{L(l)} C_{2AX}^{R(l)*} \frac{-3+4x_{AX}-x_{AX}^2-2\ln x_{AX}}{(1-x_{AX})^3} + (L \leftrightarrow R), \quad (\text{C3})$$

where $x_{AX} = M_{\tilde{\chi}_A^-}^2 / m_{\tilde{\nu}_X}^2$.

The neutralino-loop contribution $g_\mu^{(N)}$ is

$$g_\mu^{(N)} = -\frac{1}{48\pi^2} \frac{m_\mu^2}{m_{\tilde{l}_X}^2} |N_{2AX}^{L(l)}|^2 \frac{1-6x_{AX}+3x_{AX}^2+2x_{AX}^3-6x_{AX}^2\ln x_{AX}}{(1-x_{AX})^4} - \frac{1}{16\pi^2} \frac{m_\mu M_{\tilde{\chi}_A^0}}{m_{\tilde{l}_X}^2} N_{2AX}^{L(l)} N_{2AX}^{R(l)*} \frac{1-x_{AX}^2+2x_{AX}\ln x_{AX}}{(1-x_{AX})^3} + (L \leftrightarrow R), \quad (\text{C4})$$

where $x_{AX} = M_{\tilde{\chi}_A^0}^2 / m_{\tilde{l}_X}^2$.

-
- [1] T. Yanagida, in *Proceedings of the Workshop on Unified Theory and Baryon Number of the Universe*, Tsukuba, Japan, 1979, edited by O. Sawada and A. Sugamoto (KEK Report No. 79-18, Tsukuba, 1979), p. 95; M. Gell-Mann, P. Ramond, and R. Slansky, in *Supergravity*, Proceedings of the Workshop, Stony Brook, New York, 1979, edited by P. van Nieuwenhuizen and D. Freedman (North-Holland, Amsterdam, 1979).
- [2] F. Borzumati and A. Masiero, Phys. Rev. Lett. **57**, 961 (1986).
- [3] J. Hisano, T. Moroi, K. Tobe, M. Yamaguchi, and T. Yanagida, Phys. Lett. B **357**, 579 (1995).
- [4] K. Inoue, A. Kakuto, H. Komatsu, and S. Takeshita, Prog. Theor. Phys. **68**, 927 (1982).
- [5] For a review, see H.P. Nilles, Phys. Rep. **C110**, 1 (1984).
- [6] J.C. Sen, Phys. Rev. **113**, 679 (1959); K.W. Ford and J.G. Wills, Nucl. Phys. **35**, 295 (1962); R. Pla and J. Bernabéu, Ann. Fis. (Leipzig) **67**, 455 (1971); H.C. Chiang, E. Oset, T.S. Kosmas, A. Faessler, and J.D. Vergados, Nucl. Phys. **A559**, 526 (1993).
- [7] J. Bernabeu, E. Nardi, and D. Tommasini, Nucl. Phys. **B409**, 69 (1993), and references therein.
- [8] Particle Data Group, L. Montanet *et al.*, Phys. Rev. D **50**, 1173 (1994).
- [9] J. Gasser and H. Leutwyler, Phys. Rep. **87**, 77 (1982).
- [10] M. Bando, T. Kugo, N. Maekawa, and H. Nakano, Mod. Phys. Lett. A **7**, 3379 (1992).
- [11] D.A. Kosower, L.M. Krauss, and N. Sakai, Phys. Lett. **133B**, 305 (1983); T.C. Yuan, R. Arnowitt, A.H. Chamseddine, and P. Nath, Z. Phys. C **26**, 407 (1984).
- [12] U. Chattopadhyay and P. Nath, Phys. Rev. D **53**, 1648 (1996). and references therein.
- [13] J.L. Lopez, D.V. Nanopoulos, X. Wang, and A. Zichichi, Phys. Rev. D **51**, 147 (1995); T. Goto and Y. Okada, Prog. Theor. Phys. **94**, 407 (1995); G. V. Kraniotis, Report No. SUSX-TH-95-15, hep-ph/9507432 (unpublished).
- [14] B. de Carlos and J.A. Casas, Phys. Lett. B **349**, 300 (1995); **351**, 604(E) (1995).
- [15] J.G. Learned, S. Pakvasa, and T.J. Weiler, Phys. Lett. **207**, 79 (1988).
- [16] T. Moroi, Phys. Lett. B **321**, 56 (1994).
- [17] R. Barbieri and L.J. Hall, Phys. Lett. B **338**, 212 (1994).
- [18] R. Barbieri, L.J. Hall, and A. Strumia, Nucl. Phys. **B445**, 219 (1995).
- [19] P. Ciafaloni, A. Romanino, and A. Strumia, Report No. IFUP-TH-42-95, hep-ph/9507379 (unpublished); N. Arkani-Hamed, S.-C. Cheng, and L.J. Hall, Phys. Rev. D. **53**, 413 (1995).